9.09 Thermal and Compositional Evolution of the Core

F. Nimmo, University of California, Santa Cruz, CA, USA

9.09.1 Introduction

The evolution of the Earth's core is important for three main reasons. First, the formation of the core was one of the central events in the ancient, but geologically rapid, period over which the Earth accreted, and generated observational constraints on this poorly understood epoch. Second, the initial conditions, both thermal and compositional, established during this period have largely controlled the subsequent evolution of the core, and may have also significantly affected the mantle. Finally, the evolution of the Earth's core resulted in the generation of a long-lived global magnetic field, which did not occur for the superficially similar cases of Mars or Venus. The objective of this chapter is to describe our current understanding of the evolution of the core, from shortly after its formation to the present day.

The first section of this chapter will summarize the present-day state of the core, since it is this state which is the end product of the core's evolution. The bulk of the chapter will then examine how the core evolved from its initial thermal and compositional state. Most of the arguments will be based on physics rather than chemistry, as compositional constraints on the core's long-term evolution are rare and often controversial.

The material covered in this chapter follows on directly from the chapter by Chapter 9.03, in which the origin and formation of the core are discussed. Much of the discussion of the core's energy and entropy budgets is derived from a more thorough treatment in Chapter 8.02. Other aspects of the core's

behavior are described in chapters in this treatise by Chapters 8.05, 8.06, 8.03, 8.08, and 8.09. The companion *Treatise on Geochemistry* contains useful articles on planetary accretion (Chambers, 2003) and various aspects of core composition (Righter and Drake, 2003; Li and Fei, 2003; McDonough, 2003).

9.09.2 Present-Day State of the Core

Prior to investigating the earliest history and evolution of the core, it is important to briefly describe its present-day features. More detail can be found in the chapters referred to above; here the focus is on those parameters which are most important when considering the thermal and compositional evolution of the core. In particular, the uncertainties associated with these parameters will be assessed; doing so is important when assessing the likely range of thermal evolution outcomes (Section 9.09.3.2). The values and uncertainties adopted are discussed below and in more detail in Chapter 8.02; they are based on those used in previous investigations by Buffett *et al.* (1996), Roberts *et al.* (2003), Labrosse (2003), and Nimmo *et al.* (2004).

9.09.2.1 Density and Pressure

The radially averaged density structure of the core may be derived directly from seismological observations. The density of the core increases monotonically with depth, due to the increasing pressure. However, there is also a sharp density discontinuity at the inner-core boundary (ICB), which arises because of two effects. First, solid core material is inherently denser than liquid core material at the same pressure and temperature (P, T) conditions. Second, the outer core contains more of one or more light elements than the inner core (e.g., Poirier, 1994; McDonough, 2003), and would therefore be less dense even if there were no phase change. This compositional density contrast $\Delta\rho_c$ has a dominant role in driving compositional convection in the core; unfortunately, its magnitude is uncertain by a factor ≈ 2.

The total density contrast across the ICB is somewhat uncertain. A recent normal mode study (Masters and Gubbins, 2003) gives a total density contrast of 640–1000 kg m^{-3}, or 5.3–8.3%, which agrees rather well with the result of 600–900 kg m^{-3} obtained using body waves (Cao and Romanowicz, 2004), but is somewhat higher than the value obtained by Koper and Dombrovskaya (2005). The density contrast between pure solid and liquid Fe at the ICB is estimated at 1.8% (Alfe *et al.*, 1999). These results imply a compositional density contrast of 3.5–6.5%, or $\Delta\rho_c = 400$–$800\,\mathrm{kg\,m^{-3}}$, and may in turn be used to estimate the difference in light element(s) concentrations between inner and outer core, which helps to sustain the dynamo (see Section 9.09.3.2.2).

For the theoretical models described later (Section 9.09.3), it is important to have a simple description of the density variation within the Earth. One such description is given by Labrosse *et al.* (2001), where the variation of density ρ with radial distance r from the centre of the Earth is given by

$$\rho(r) = \rho_{\mathrm{cen}} \exp\left(-r^2/L^2\right) \quad [1]$$

where ρ_{cen} is the density at the center of the Earth and L is a length scale given by

$$L = \sqrt{\frac{3K_0(\ln(\rho_{\mathrm{cen}}/\rho_0) + 1)}{2\pi G\rho_0\rho_{\mathrm{cen}}}} \quad [2]$$

Here K_0 and ρ_0 are the compressibility and density at zero pressure, respectively, G is the universal gravitational constant and $L = 7272$ km using the parameters given in Chapter 8.02. Although this expression neglects the density jump at the ICB, the error introduced is negligible compared to other uncertainties.

The corresponding pressure is given by

$$P(r) = P_c + \frac{4\pi G\rho_{\mathrm{cen}}^2}{3}\left[\left(\frac{3r^2}{10} - \frac{L^2}{5}\right)\exp\left(-r^2/L^2\right)\right]_r^R \quad [3]$$

where P_c is the pressure at the CMB and R is the core radius.

9.09.2.2 Thermodynamic Properties

From the point of view of the thermal evolution of the core, the most important parameters are those which determine the temperature structure and heat flux within the core, in particular the thermal conductivity k and expansivity α (see Section 9.09.2.4).

The thermal conductivity of iron at core conditions is obtained by using shock-wave experiments and converting the measured electrical conductivity to thermal conductivity using the Wiedemann–Franz relationship (Stacey and Anderson, 2001). The canonical value for k at the CMB of 46 W m^{-1} K^{-1} (Stacey and Anderson, 2001) was based on shock measurements by Matassov (1977). More recent shock experiments by Bi *et al.* (2002) suggest a

conductivity closer to 30 W m^{-1} K^{-1}. Here a value of 40 ±20 W m^{-1} K^{-1} as spanning the likely uncertainties is assumed.

The thermal expansivity within the core may be obtained from seismology if the Gruneisen parameter is known. Recent results suggest that this parameter remains constant at roughly 1.5 throughout the core (e.g., Anderson, 1998; Alfe *et al.*, 2002b). Because the seismic parameter increases with depth, α increases by a factor of 1.5–2 from the center of the Earth to the CMB (Labrosse, 2003; Roberts *et al.*, 2003), but little accuracy is sacrificed if a constant mean value of α is adopted. Following the latter two authors, in this chapter a range $(0.8–1.9) \times 10^{-5}$ K^{-1} is adopted. A list of estimated values for important parameters is given in **Table 2**; more details may be found in Chapter 8.02.

9.09.2.3 Composition

The composition of the core is important because it potentially provides constraints on its origin and mode of formation. Unfortunately, as will be seen below, the constraints provided are currently rather weak, as few elements have well-known core abundances.

9.09.2.3.1 Light elements

It is clear from seismology and experiments that the outer core is 6–10% less dense than pure liquid iron would be under the estimated P, T conditions (e.g., Alfe *et al.*, 2002a). While the core almost certainly contains a few weight percent nickel (e.g., McDonough, 2003), this metal has an almost identical density to iron and is thus not the source of the density deficit (e.g., Li and Fei, 2003). The inner core also appears to be less dense than a pure iron composition would suggest (Jephcoat and Olson, 1987), though here the difference is smaller. Both the outer and inner core must therefore contain some fraction of light elements, of which the most common suspects are sulfur, silicon, oxygen, carbon, and hydrogen (see Poirier (1994), Hillgren *et al.* (2000), and Li and Fei (2003) for reviews). For any particular element, or mixture of them, the inferred density deficit may be used to infer the molar fraction of the light element(s) present. Because the density deficit is larger in the outer core, it is thought that light elements are being expelled during crystallization of the inner core. This expulsion is of great importance, because it generates compositional convection which helps to drive the geodynamo (see Section 9.09.3.2.2).

Apart from their role in driving the dynamo, these light elements are important for two other reasons. First, they probably reduce the melting temperature of the core by several hundred degrees kelvin (see Section 9.09.2.4). Second, if the actual light elements in the core could be reliably identified, they would provide a strong constraint on the conditions under which the core formed.

Table 1 gives several examples of model core compositions. All these models are derived by comparing estimates of the bulk silicate Earth elemental abundances (inferred from upper-mantle nodules and crustal samples), with estimates of the initial solar nebular composition (based mainly on chondritic meteorite samples). Although there is some agreement on the abundances of Fe, Ni, and Co, the relative abundances of the light elements (Si, S, O, C) vary widely. The abundance of H in the core cannot be modeled in this way because of its extreme volatility; in practice, it will be determined by the P, T conditions and amount of H in the Earth's mantle prior to and during differentiation (see, e.g., Abe *et al.* (2000) and Okuchi (1997)).

These cosmochemical models do not take into account the ease with which different elements partition into iron under the relevant conditions. Available experiments suggest that O and S can both enter the core under oxidizing conditions, while Si requires reducing conditions and is mutually incompatible with O (Kilburn and Wood, 1997; Hillgren *et al.*, 2000; Li and Fei, 2003; Malavergne *et al.*, 2004). An Fe–O–S liquid with 10.5 ±3.5 wt.% S and 1.5 ±1.5 wt.% O is also compatible with seismological observations (Helffrich and Kaneshima, 2004), although cosmochemical models do not favor such large amounts of sulfur (**Table 1**). An Fe–O–S core thus suggests core formation conditions which were relatively oxidizing (hence ruling out, for instance, the presence of substantial amounts of H in

Table 1 Model core compositions

	MA	WD	A+	McD-1	McD-2
Fe (wt.%)	84.5	80.3	79.4	85.5	88.3
Ni	5.6	5.5	4.9	5.2	5.4
Si	–	14.0	7.4	6.0	–
S	9.0	–	2.3	1.9	1.9
O	–	–	4.1	–	3.0
C	–	–	–	0.2	0.2
Co	0.26	0.27	0.25	–	–

MA = Morgan and Anders 1980; WD = Wanke and Dreibus 1988; A + = Allegre *et al.* 1995a; McD-1 and McD-2 refer to two different models given in McDonough (2003).

the core), and also relatively high temperature. These inferred conditions are roughly consistent with estimates based on mantle siderophile element abundances (*see* Chapter 9.03).

An additional constraint is that the outer core appears to contain more of the light element(s) than the inner core (Section 9.09.2.3.1). This implies that one or more of the light elements must partition strongly into liquid iron during freezing, which is potentially diagnostic behavior. For instance, Alfe *et al.* (2002a) used molecular dynamics simulations to find that oxygen, due to its small atomic radius, tends to be expelled during freezing. Conversely, S and Si have atomic radii similar to that of iron at core pressures, and thus substitute freely for iron in the solid inner core. These results thus support the case for O being one of the light elements, in agreement with the Fe–O–S core hypothesized by Helffrich and Kaneshima (2004). Unfortunately, similar models have not yet been carried out for either H or C, which might also behave in a similar manner to O. Furthermore, the results concerning S, Si, and O need additional confirmation, preferably by experiments. Nonetheless, the implications for core formation and composition are potentially important.

For completeness, it is noted that some other gases, such as nitrogen (Adler and Williams, 2005) and xenon (Lee and Steinle-Neumann 2006), may also partition into the core. However, other studies have found negligible partitioning (Matsuda *et al.*, 1993; Ostanin *et al.*, 2006). More to the point, since neither the initial abundance of such gases, nor their current concentrations in the core, are currently known, they do not in general provide any constraints on core evolution.

9.09.2.3.2 Radioactive isotopes

Although the bulk of the core consists of Fe, Ni and a few weight percent light elements, some trace elements are also of importance. First, the radioactive isotopes of K, Th, and U can potentially have a significant effect on both the age of the inner core and the maintenance of the dynamo (e.g., Labrosse *et al.*, 2001; Buffett, 2002; Nimmo *et al.*, 2004). Unfortunately, there is as yet little agreement on whether or not such elements are really present in the core. Longer discussions on this issue may be found in McDonough (2003) and Roberts *et al.* (2003); only a brief summary is given here, while the role of radioactive elements in core evolution is discussed in Section 9.09.3.2.

There is little evidence, either from cosmochemistry or partitioning experiments, to expect either U or Th to partition into the core. On the other hand, the Earth's mantle is clearly depleted in K relative to chondrites (e.g., Lassiter 2004). However, since K is a volatile element, it is unclear whether this depletion is due to sequestration of K in the core, or simple loss of K from the Earth as a whole early in its history. Experimental investigations (Gessmann and Wood, 2002; Murthy *et al.*, 2003) show that partitioning of K into core materials is possible, but also depends in a complex fashion on other factors such as the amount of sulfur present. The removal of K to the core would also likely involve the removal of other elements with similar affinities for iron, but it is not yet clear what constraints the observed abundances of these other elements place on the amount of K in the core. It currently appears that up to a few hundred ppm K in the core is permitted, but not required, by both the experiments and the geochemical observations. The detection of antineutrinos produced by radioactive decay in the Earth's interior (Araki *et al.*, 2005) may help to ultimately resolve this question.

A second set of potentially very important isotopes are those of osmium, because they may constrain the onset of inner-core formation (e.g., Walker *et al.*, 1995). The arguments for and against this somewhat controversial hypothesis are discussed in Section 9.09.3.3.1. The reason the arguments are important is that the onset of inner-core formation is currently very poorly constrained by theoretical models (Section 9.09.3.2.5); thus, the addition of an observational constraint would significantly improve our understanding of the core's evolution.

A final important isotopic system is ^{182}Hf–^{182}W. This system permits the age of core formation to be deduced (e.g., Harper and Jacobsen, 1996; Kleine *et al.*, 2002; Nimmo and Agnor, 2006) and is discussed in some detail in Chapter 9.03. Other isotopic systems can potentially be used in similar ways (see Allegre *et al.* (1995b)). However, the Pd–Ag system is experimentally very challenging (Carlson and Hauri, 2001), and the U–Pb system suffers from the potential loss of lead due to its high volatility (e.g., Halliday, 2004).

9.09.2.4 Temperature Structure

Both the temperature structure within the core, and the shape of the melting curve, play an important role in determining the thermal evolution of the core. As long as the core is convecting, its mean temperature profile will be that of an adiabat, except at the very thin top and bottom boundary layers. Since the temperature at the ICB must equal the melting

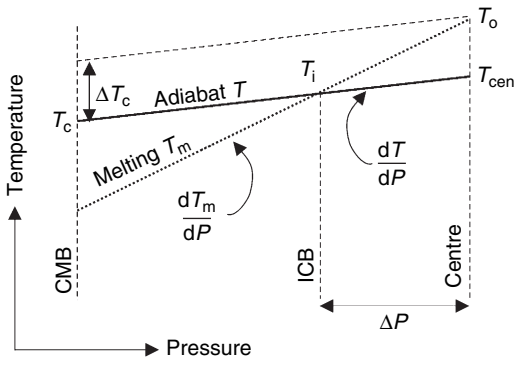

Figure 1 Definition sketch for temperature structure within the core. Note that in reality neither temperature profile is linear.

temperature of the core at that pressure (**Figure 1**), the temperature elsewhere in the core may be extrapolated from the ICB conditions by using the appropriate adiabat. Thus, determining the melting behavior of core material is crucial to establishing the temperature structure of the core.

The adiabatic temperature T within the core is given by (Labrosse *et al.*, 2001)

$$T(r) = T_{cen} \exp\left(-r^2/D^2\right) \quad [4]$$

where T_{cen} is the temperature at the center of the Earth and D is a length scale given by

$$D = \sqrt{3C_p/2\pi\alpha\rho_{cen}G} \quad [5]$$

Here C_p is the specific heat capacity, α is the thermal expansivity (Section 9.09.2.2) and $D = 5969$ km using the parameters given in **Table 2**, model 2.

The melting behavior of pure iron is difficult to establish: experiments at the P, T conditions required (e.g., Brown and McQueen, 1986; Yoo *et al.*, 1993; Boehler, 1993) are challenging, and computational (first-principles) methods (e.g., Laio *et al.*, 2000; Belonoshko *et al.*, 2000; Alfe *et al.*, 2002b) are time-consuming and hard to verify. Furthermore, the presence of the light element(s) likely reduces the melting temperature from that of pure iron, but by an uncertain amount. These issues are discussed in detail elsewhere in this volume (Chapter 8.02), and only a summary is provided here.

Based on first-principles calculations, Alfe *et al.* (2003) predict a temperature at the ICB T_i of 5650 ± 600 K, taking into account the reduction in temperature due to the light element(s). The gradient in melting temperature is roughly 8.5 K GPa^{-1} at the ICB. These results are broadly consistent with the low-pressure diamond anvil cell results of Shen *et al.* (1998) and Ma *et al.* (2004), though not those of Boehler (1993). Similarly, the results agree with the higher-pressure shock-wave results of Brown and McQueen (1986) and Nguyen and Holmes (2004), though not those of Yoo *et al.* (1993). The numerical results of Belonoshko *et al.* (2000) and Laio *et al.* (2000) also give similar answers once corrections due to the different molecular dynamics techniques used have been applied. Further discussions of the differing results and the reliability of different theoretical approaches may be found in Alfe *et al.* (2004) and Bukowinski and Akber-Knutson (2005).

Given the ICB temperature and the relevant thermodynamic quantities, the temperature at the core side of the CMB, T_c, may be deduced and is approximately 4000 K. This value is actually of only secondary importance as far as the thermal evolution of the core is concerned; of much greater interest are

Table 2 Parameter values adopted

	Model						Model				
	1	2	3	Units	Eq.		1	2	3	Units	Eq.
k	20	40	60	W m^{-1} K^{-1}	2.2	$\Delta\rho_c$	600	400	200	kg m^{-3}	2.1
ΔT_c	150	100	50	K	(7)	α	0.8	1.35	1.9	$\times 10^{-5}$ K^{-1}	(5)
D	7754	5969	5031	km	(5)	T_{cen}	4893	5619	6454	K	(4)
T_i	4773	5389	6085	K	2.4	T_o	5076	5760	6535	K	2.4
T_{m0}	1460	1322	1165	K	(6)	dT_m/dP	10.1	12.4	15.0	K GPa^{-1}	(6)
Q_k	1.4	4.8	10.0	TW	(12)	$\tilde{Q}_T$	2.9	3.2	3.8	$\times 10^{27}$ J	(11)

Eq. is the equation or section in which each parameter is defined.
Models 1 and 3 are end-member cases using parameter values designed to generate ancient and recent inner cores, respectively; model 2 is a best guess at the real parameter values. Variables below the horizontal line have values derived from the initial parameter choices (k, α,$\Delta\rho_c$, ΔT_c). Other parameters not specified here are assumed constant in all three models and are generally the same as those adopted in 00128. In particular, $T_c = 4000$ K, latent heat $L_H = 750$ kJ kg^{-1}, $C_p = 840$ J kg^{-1} K^{-1}, $\rho_{cen} = 12\,500$ kg m^{-3}.

the relative slopes of the adiabat and the melting curve (see below).

Although more complicated approaches may be adopted (e.g., Buffett *et al.*, 1996; Labrosse *et al.*, 2001; Roberts *et al.*, 2003), a reasonable approximation is that the core melting temperature is simply a linear function of pressure. Thus, the core melting temperature T_m may be written as

$$T_m(P) = T_{m0} + \frac{dT_m}{dP} P \qquad [6]$$

where dT_m/dP and T_{m0} are constants and T_{m0} incorporates the reduction in melting temperature due to the light element(s). Note that this linearization is only intended to work over the core pressure range, and that T_{m0} thus does not represent the actual zero-pressure melting temperature.

When considering the growth history of the inner core, the crucial parameter is the difference in gradients between the melting curve and the adiabat. One way of expressing this quantity is to define ΔT_c, the change in the CMB temperature since the onset of inner-core solidification. As shown in **Figure 1**, ΔT_c may be defined as follows:

$$\begin{aligned}\Delta T_c &= \frac{\Delta P}{f_{ad}}\left(\frac{dT_m}{dP} - \frac{dT}{dP}\right) \\ &= 22\,K\left(\frac{dT_m/dP - dT/dP}{1\,K\,GPa^{-1}}\right)\end{aligned} \qquad [7]$$

where ΔP is the pressure difference between the present ICB and the center of the Earth, T and T_m are the adiabatic and melting temperatures, respectively, f_{ad} is a factor converting the temperature at the CMB to that at the ICB and the curves are assumed linear over the relevant pressure range. The numerical values are obtained from model 2 in **Table 2**. Because the adiabatic and melting gradients are both uncertain and of similar sizes, the uncertainty in ΔT_c tends to be amplified. Values for ΔT_c from four recent studies (Buffett *et al.*, 1996; Roberts *et al.*, 2003; Labrosse, 2003; Nimmo *et al.*, 2004) range from 31–146 K, with smaller values implying younger inner cores (*see* Chapter 8.02). Here I assume a range of 50–150 K as representative of the likely uncertainties. By choosing values for T_c, ΔT_c and the adiabatic gradient, the ICB temperature T_i and dT_m/dP are then specified (see **Table 2**). Note that the melting gradients obtained exceed the value given by Alfe *et al.* (2003); a reduction in this gradient would result in a smaller ΔT_c (eqn [7]) and thus a younger inner core. Hence, the range of values for ΔT_c chosen here is conservative.

9.09.2.5 The CMB Region

The CMB region is relevant to core evolution for two reasons. First, it is the behavior of this region, and in particular its temperature structure, which controls the rate at which heat is extracted from the core. As a consequence, the thermal evolution of the core is intimately tied to that of the mantle. This interdependence between the core and mantle is one of the reasons that theoretical investigations of core thermal evolution are subject to such large uncertainties.

Second, the CMB region is interesting from a compositional point of view, since it is the point at which regions containing elements with very different chemical potentials meet. The extent to which the resulting reactions have influenced the behavior of the deepest mantle (or the outermost core) is unclear. However, because these reactions provide indications of core evolution, the question of whether core or CMB material can plausibly be entrained to the surface is of considerable interest (Section 9.09.3.3.2).

Whether or not a dynamo can be sustained ultimately depends on the CMB heat flow, that is, the rate at which heat is extracted from the core (Section 9.09.3.2.2). The CMB heat flow, in turn, is determined by the ability of the mantle to remove heat. Importantly, independent estimates on this cooling rate exist, based on our understanding of mantle behavior.

One approach to estimating the heat flow across the base of the mantle relies on the conduction of heat across the bottom boundary layer. As discussed in Section 9.09.2.4, the temperature at the bottom of this layer (the core) arises from extrapolating the temperature at the ICB outwards along an adiabat, and is about 4000 K. The temperature at the top of the layer is obtained from extrapolating the mantle potential temperature inwards along an adiabat, and is about 2700 K (Boehler, 2000). Williams (1998) concluded that the likely temperature contrast across the CMB is 1000–2000 K. Based on seismological observations, the thickness of D'', which might represent a thermal boundary layer, is 100–200 km. For likely lower-mantle thermal conductivities, the resulting conductive heat flow is probably in the range 9 ± 3 TW (Buffett, 2003). Unfortunately, as discussed below, the CMB region is complicated enough that this simple estimate may not be robust.

A second method of estimating CMB heat flow is to add up the near-surface contributions from

inferred convective plumes (Davies, 1988; Sleep, 1990). These early estimates gave heat flows a factor of 2–4 smaller than the simple conductive argument. However, it is now becoming clear that these estimates are probably too low, both because the temperature contrast between plumes and the background mantle varies with depth (Bunge, 2005; Zhong, 2006; Mittelstaedt and Tackley, 2006) and because not all plumes may reach the surface (Labrosse, 2002). Two recent theoretical studies of convection including, respectively, compositional layering and the postperovskite phase transition result in CMB heat flows of ~13 TW (Zhong, 2006) and 7–17 TW (Hernlund *et al.*, 2005).

One additional complication is that D'' may contain enhanced concentrations of radioactive elements (e.g., Coltice and Ricard, 1999; Tolstikhin and Hofmann, 2005; Boyet and Carlson, 2005). In this case, the heat flow out of the core will be less than the heat flows inferred from the models of Zhong (2006) and Hernlund *et al.* (2005). Bearing this caveat in mind, these model results are roughly consistent with the simple conductive heat flow estimate, and suggest that a range of 10 ± 4 TW is likely to encompass the real present-day CMB heat flow. This range of heat flows suggests a current core cooling rate dT_c/dt of 65–150 K Gy^{-1}, using the parameters for model 2.

The compositional nature of the CMB region may also have an effect on the evolution of the core. The CMB region may be at least partially molten, an inference supported by the presence of a (laterally discontinuous) ultralow velocity zone (e.g., Garnero *et al.*, 1998). The presence of such a melt layer, which is probably denser than the surrounding solid material (Knittle, 1998; Akins *et al.*, 2004), is likely to affect heat transfer from the core to the mantle. Such a layer is also likely to have been more extensive in the past, when core temperatures were higher (see Section 9.09.3.2.6 and Chapter 9.03). Another possibility is the presence of high-density, compositionally distinct material, probably subducted oceanic crust. Again, this material, especially if enriched in radioactive materials (Buffett, 2002), is likely to have affected long-term core evolution (Nakagawa and Tackley, 2004a). Finally, the CMB region may include a phase transition to a postperovskite structure (e.g., Murakami *et al.*, 2004), which will also affect the CMB heat flux (Nakagawa and Tackley, 2004b; Hernlund *et al.*, 2005). The manner in which the CMB may have evolved with time in response to the evolution of the core is discussed further in Section 9.09.3.3.2.

9.09.2.6 Dynamo Behavior Over Time

One might expect that the behavior of the Earth's magnetic field over time would provide information on the evolution of the dynamo and core. However, despite much work on this subject (see reviews by Jacobs (1998) and Valet (2003)), the information is limited to the following: (1) a reversing, predominantly dipolar field has existed, at least intermittently, for at least the last 3.5 Gy; (2) the amplitude of the field does not appear to have changed in a systematic fashion over time.

There are several reasons why there are so few constraints. First, the magnetic field that we can measure at the surface is different in both frequency content and amplitude from the field within the core. In particular, ohmic heating is dominated by small-scale magnetic fields which are not observable at the surface (see below). Second, the number of observations on paleomagnetic fields decline dramatically prior to ≈150 My BP because of the almost complete absence of unsubducted oceanic crust. Third, there is little theoretical understanding of how changes in core behavior relate to changes in the observed magnetic field.

The first two problems are unlikely to be resolved in the forseeable future. However, there has been some progress with the third, thanks to increasingly realistic simulations of the geodynamo (see reviews by Busse (2000), Glatzmaier (2002), Kono and Roberts (2002), and Chapter 8.08, and a recent paper by Olson and Christensen (2006)). In particular, a study by Roberts and Glatzmaier (2001) found that increasing the inner-core size tended to result in a less axisymmetric field and (surprisingly) greater time variability. Thus, at least in theory, observed changes in the time variability of the magnetic field with time could be used to place constraints on the evolution of the Earth's core. An observed variation in the amplitude with time (e.g., Labrosse and Macouin, 2003), however, is less likely to be useful: Roberts and Glatzmaier (2001) found that models with inner cores 0.25 and 2 times the radii of the current inner core both produced similar mean field amplitudes, and a similar result was found by Bloxham (2000). Furthermore, it is not clear that changes in global variables, such as core cooling rate or inner core size, will have a larger effect on the field behavior than local factors such as the heat flux boundary condition (e.g., Christensen and Olson, 2003).

In spite of the difficulties in extracting detailed information on core evolution from the paleomagnetic record, an important result is that the geodynamo appears to have persisted, without long-term interruptions, for at least 3.5 Gy (McElhinny and Senanayake, 1980). The pattern of magnetic reversals for the Proterozoic is well known, but not well understood. For instance, although reversals occur roughly every 0.25 My on average (Lowrie and Kent, 2004), there were no reversals at all in the period 125–85 Ma, for reasons which are obscure but may well have to do with the behavior of the mantle over that interval (e.g., Glatzmaier *et al.*, 1999). The earliest documented apparent paleomagnetic reversal is at 3.2 Gy BP (Layer *et al.*, 1996). Although the amplitude of the field has varied with time (Selkin and Tauxe, 2000; Prevot *et al.*, 1990), the maximum field intensity appears never to have exceeded the present-day value by more than a factor of 5 (Valet, 2003; Dunlop and Yu, 2004).

In summary, the fact that a reversing dynamo has apparently persisted for >3.5 Gy can be used to constrain the evolution of the core over time (see Section 9.09.3.2 below). Unfortunately, other observations which might potentially provide additional constraints, such as the evolution of the field intensity, are either poorly sampled or difficult to relate to the global energy budget, or both.

9.09.2.6.1 Ohmic dissipation

As discussed below, the power dissipated in the core by ohmic heating is a critical parameter to determining whether a dynamo can operate: a more dissipative dynamo requires more rapid core cooling and a higher CMB heat flux. Unfortunately, this heating rate is currently very poorly constrained. The heating is likely to occur at length scales which are sufficiently small that they can neither be observed at the surface, nor resolved in numerical models (Roberts *et al.*, 2003). Moreover, the toroidal field, which is undetectable at the surface, may dominate the heating.

The ohmic dissipation Q_Φ may be converted to an entropy production rate E_Φ using $E_\Phi = Q_\Phi / T_D$ (Roberts *et al.*, 2003), where the characteristic temperature T_D is unknown but intermediate between T_i and T_c and is here assumed to be 5000 K. The entropy production rate is simply a convenient way of assessing the potential for generating a dynamo, and is discussed in more detail in Section 9.09.3.2.2 and Chapter 8.02. One approach to estimating the required rate is to extrapolate from numerical dynamo simulations. Roberts *et al.* (2003) used the results of the Glatzmaier and Roberts (1996) simulation to infer that 1–2 TW are required to power the dynamo, equivalent to an entropy production rate of 200–400 MW K^{-1}. The dynamo model of Kuang and Bloxham (1997) gives an entropy production rate of 40 MW K^{-1}. Christensen and Tilgner (2004) gave a range of 0.2–0.5 TW, based on numerical and laboratory experiments, equivalent to 40–100 MW K^{-1}, and Buffett (2002) suggested 0.1–0.5 TW, equivalent to 20–100 MW K^{-1}. Labrosse (2003) argues for a range 350–700 MW K^{-1}, and Gubbins *et al.* (2003) favor 500–800 MW K^{-1}. We shall regard the required ohmic dissipation rate as currently unknown, but think it likely that entropy production rates in excess of 50 MW K^{-1} are sufficient to guarantee a geodynamo.

9.09.2.7 Summary

The present-day temperature structure and composition of the core establish boundary conditions which constrain both the core's initial mode of formation, and subsequent evolution. In particular, the size of the inner core and the persistence of the geodynamo for at least 3.5 Gy place constraints on the CMB heat flux. Light elements in the Earth's core not only help to power the dynamo, but also constrain the conditions under which the Earth formed. Radioisotopes are a potential additional source of power, and also provide the ability to date core formation and (potentially) constrain the age of the inner core.

The next section will examine how the core evolved from the initial conditions established by the accretion process to its inferred present-day state.

9.09.3 Evolution of the Core

9.09.3.1 Formation and Initial State

The initial thermal and chemical conditions of the Earth's core were determined by the manner in which the Earth accreted, a relatively geologically rapid process. This period of the core's history is discussed extensively in Chapter 9.03 and only a brief summary is given here.

Theoretical arguments and geochemical observations suggest that the Earth accumulated the bulk of its mass through a few, large impacts within about 50 My of solar system formation, and that each of these impacts generated a global, if transient, magma

ocean. Although the impacting bodies were undoubtedly differentiated, pre-existing chemical signals appear to have been overprinted by the impact process. Siderophile element concentrations are consistent with a magma ocean extending to mid-mantle depths (500–1000 km, 2000–3000 K). The impactor cores likely underwent emulsification as they traversed the magma ocean, resulting in near-complete chemical re-equilibration. This re-equilibration ceased as the metal pooled at the base of the magma ocean; subsequent transport of the resulting large-scale iron masses to the pre-existing core was rapid and resulted in increased core temperatures. Following the Moon-forming impact, the initial core temperature was probably at least 5500 K, suggesting extensive melting in the lowermost mantle.

After this initial period of large and geologically rapid transfers of mass and energy, the subsequent thermal and compositional evolution of the core – the focus of this section – was much less dramatic. Unfortunately, there are few observational constraints on the details of this longer-term evolution. As discussed below, present-day observations (in particular, the size of the inner core and estimates of the CMB heat flux) provide some constraints. The fact that a geodynamo has apparently operated for at least 3.5 Gy provides a lower bound on the rate at which the core must have cooled. However, it is important to note that the long-lived field does not necessarily require a similarly ancient inner core. Isotopic signals, however, may provide a constraint on the inner core age, though this is highly controversial (Section 9.09.3.3.1).

The first half of this section will investigate the thermal evolution of the core. In particular, it will focus on three questions: how much has the core cooled over time?; when did the inner core start to grow?; and how was the dynamo maintained? Because of the paucity of observational constraints, this section will focus on theoretical approaches, and in particular on the uncertainties introduced by uncertainties in the relevant parameters. The subsequent section will focus on the compositional evolution of the core, in particular the chemical effects of inner-core formation, and possible reactions taking place at the CMB.

9.09.3.2 Thermal Evolution

The thermal evolution of the Earth's core has been the subject of considerable interest over the last decade. As outlined in Section 9.09.2, experimental uncertainties have led different groups to adopt different values for parameters of interest, such as the thermal conductivity. Accordingly, the calculations carried out in this section will make use of three different sets of parameters (**Table 2**): one end-member designed to maximize the likelihood of an ancient inner core (model 1); one using the best-guess parameter values (model 2); and one using values designed to minimize the inner-core age (model 3). In this way, the uncertainties involved in the theoretical calculations will be made clear, while conclusions which are robust under all three models are likely to prove durable.

9.09.3.2.1 Core cooling

In one sense, the thermal evolution of the core is relatively simple. Heat is extracted out of the core at the CMB, at a rate which depends primarily on processes within the mantle. As a result, in the absence of an internal heat source, the core cools with time. At some point, the core adiabatic crosses the melting curve, and inner-core solidification begins (**Figure 1**).

The instantaneous energy balance within the core may be written (e.g., Buffett *et al.*, 1996; Roberts *et al.*, 2003; Gubbins *et al.*, 2003; Chapter 8.02) as

$$Q_{\mathrm{cmb}} = Q_{\mathrm{s}} + Q_{\mathrm{g}} + Q_{\mathrm{L}} + Q_{\mathrm{R}} = \tilde{Q}_{\Gamma}\frac{\mathrm{d}T_{\mathrm{c}}}{\mathrm{d}t} + Q_{\mathrm{R}} \quad [8]$$

Here Q_{cmb} is the heat flow across the CMB, the core contributions Q_{s}, Q_{g}, Q_{L}, and Q_{R} are, respectively, from secular cooling, gravitational energy release, latent heat release, and radioactive decay, and the outer core is assumed to be adiabatic and homogeneous. Note that the assumption that the outer core is well-mixed and convecting throughout may not be the case if a stable conductive layer (e.g., Labrosse *et al.*, 1997) or a compositionally buoyant layer (e.g., Braginsky, 2006) develop at the top of the core.

The first three terms in eqn [8] are all proportional to the core cooling rate $\mathrm{d}T_{\mathrm{c}}/\mathrm{d}t$, where T_{c} is the core temperature at the CMB and $\tilde{Q}_{\Gamma}$ is a measure of the total energy released per unit change in core temperature. Both Q_{g} and Q_{L} depend on the inner-core size, and are zero in the absence of an inner core. This equation allows the evolution of the core temperature to be calculated if the CMB heat flux through time is known.

This energy balance has several important consequences. First, when inner-core formation begins, the same CMB heat flux results in a reduced core cooling rate, because of the extra energy terms (Q_{g}, Q_{L}). Second, the result of radioactive heating is likewise

to reduce the core cooling rate for the same CMB heat flux.

Radiogenic elements can have a strong effect on the core cooling rate, and thus the age of the inner core (e.g., Labrosse *et al.*, 2001). Rewriting eqn [8] we obtain a core cooling rate of

$$\frac{\mathrm{d}T_c}{\mathrm{d}t} = \frac{Q_{cmb} - Q_R}{\tilde{Q}_T} \qquad [9]$$

It is clear that the effect of the Q_R term is to reduce the rate of core cooling, and hence prolong the life of the inner core. This is an issue we return to below.

A major disadvantage with eqn [8] is that it does not include an ohmic dissipation term, because the transformation of kinetic energy to magnetic energy to heat occurs without changing the global energy balance (see Gubbins *et al.* (2003)). This equation is therefore not useful in determining the evolution of the geodynamo.

9.09.3.2.2 Maintaining the geodynamo

How the geodynamo is maintained has been a question of considerable interest since the initial work of Bullard (1950), Verhoogen (1961), and Braginsky (1963). The entropy balance approach described below was developed in the 1970s (Backus, 1975; Hewitt *et al.*, 1975; Gubbins, 1977; Loper, 1978; Gubbins *et al.*, 1979; Hage and Muller, 1979) and has been re-invigorated in the last few years (Braginsky and Roberts, 1995; Buffett *et al.*, 1996; Buffett, 2002; Lister, 2003; Labrosse, 2003; Roberts *et al.*, 2003; Gubbins *et al.*, 2003, 2004).

Ultimately, the geodynamo is maintained by the work done on the field by convective motions. This convection is driven partly by the extraction of heat into the overlying mantle, and partly by the fact that the resulting inner-core growth releases light elements into the base of the outer core. Thus, both thermal and compositional convection are important, with the relative contributions depending on the different parameter values adopted, in particular the size of the inner core.

Just as eqn [8] describes the energy balance in the core, an equivalent equation can be derived for the entropy balance (e.g., Roberts *et al.*, 2003; Labrosse, 2003; Lister, 2003; Gubbins *et al.*, 2003, 2004; Chapter 8.02). The latter equation does include ohmic dissipation (dissipation is nonreversible and is thus a source of entropy). The entropy may be thought of as the power divided by a characteristic temperature and multiplied by a thermodynamic efficiency factor. Different mechanisms (e.g., thermal and compositional convection) have different efficiency factors (e.g., Buffett *et al.*, 1996; Lister, 2003). Unfortunately, it is not currently understood how to relate the entropy production rate to global magnetic field characteristics, such as reversal frequency (Section 9.09.2.6).

The entropy rate available to drive the dynamo may be written as (e.g., Labrosse, 2003; Gubbins *et al.*, 2004)

$$\begin{aligned}\Delta E &= E_S + E_L + E_g + E_H + E_R - E_k \\ &= \tilde{E}_T \frac{\mathrm{d}T_c}{\mathrm{d}t} + E_R - E_k \end{aligned} \qquad [10]$$

where E_s, E_L, E_g, and E_H are the contributions due to cooling, latent heat and gravitational energy release and heat of reaction, respectively, E_R depends on the presence of radioactive elements in the core, and E_k depends on the adiabatic heat flux at the CMB. The first four terms are all proportional to the core cooling rate $\mathrm{d}T_c/\mathrm{d}t$, and $\tilde{E}_T$ is simply a convenient way of lumping these terms together. This equation illustrates two important points. First, as expected, a higher cooling rate or a higher rate of radioactive heat production increases the entropy rate available to drive a dynamo. Second, a larger adiabatic contribution (e.g., higher thermal conductivity) reduces the available entropy.

By combining eqns [8] and [10], an expression may be obtained which gives the core heat flow required to sustain a dynamo characterized by a particular entropy production rate E_Φ:

$$Q_{cmb} = Q_R\left(1 - \frac{T_T}{T_R}\right) + T_T(E_\Phi + E_k) \qquad [11]$$

where T_R is the effective temperature such that $T_R = Q_R/E_R$ and likewise $T_T = \tilde{Q}_T/\tilde{E}_T$. This equation encapsulates the basic physics of the dynamo problem.

Equation [11] shows that larger values of adiabatic heat flow or ohmic dissipation require a correspondingly higher CMB heat flow to drive the dynamo, as would be expected. In fact, in the absence of radiogenic heating, the CMB heat flow required is directly proportional to $E_k + E_\Phi$. The constant of proportionality depends on the thermodynamic efficiency of the core, which increases if an inner core is present. Because the term $\left(1 - (T_T/T_R)\right)$ exceeds zero, a dynamo which is partially powered by radioactive decay will require a greater total CMB heat flow than the same dynamo powered without radioactivity. Alternatively, if the CMB heat flow stays

constant, then an increase in the amount of radioactive heating reduces the entropy available to power the dynamo.

Equation [11] also illustrates the fact that a dissipative dynamo can exist even if the CMB heat flow is less than that conducted along the adiabat (i.e., subadiabatic) (Loper, 1978). In the absence of radioactivity, the entropy production rate E_Φ available for the dynamo is $(Q_{cmb}/T_T) - E_k$ which for the present-day core exceeds zero unless Q_{cmb} is strongly subadiabatic. Thus, a subadiabatic CMB heat flow can sustain a dynamo, as long as an inner core is present to drive compositional convection (e.g., Loper, 1978; Labrosse *et al.*, 1997). It should be noted that these results assume that the CMB heat flux does not vary in space; lateral variations in the heat flux may allow a dynamo to function even if the mean value of Q_{cmb} suggests that the dynamo should fail.

In the absence of an inner core and radiogenic heating, it may be shown that

$$Q_{cmb} = Q_k\left(1 + \frac{E_\Phi}{E_k}\right) \quad [12]$$

This equation shows that the heat flow at the CMB Q_{cmb} must exceed the adiabatic heat flow Q_k for a dynamo driven only by thermal convection to function. This result is important, because it demonstrates that there is no problem with sustaining a dynamo prior to the onset of inner-core formation, as long as the core cooling rate (or CMB heat flux) is large enough. This equation also allows dynamo dissipation to be taken into account explicitly: a more strongly dissipative core dynamo requires a more superadiabatic CMB heat flow to operate.

9.09.3.2.3 Present-day energy budget

Figure 2 shows how the rate of entropy production available to drive a dynamo varies as a function of the heat flow out of the core, both for a set of core parameters appropriate to the present-day Earth, and for a situation in which the inner core has not yet formed. **Figure 2(a)** illustrates the case for the best-guess parameters (model 2) while **Figure 2(b)** uses parameters designed to maximize the inner-core age (model 1). As expected, higher core heat fluxes generate higher rates of entropy production; also, the same cooling rate generates more excess entropy when an inner core exists than when thermal convection alone occurs.

As discussed above, when an inner core is present, positive contributions to entropy production arise from core cooling, latent heat release, and gravitational energy; the adiabatic contribution is negative (eqn [10]). For a present-day, radionuclide-free core, CMB heat flows of <2 TW and <0.2 TW result in negative entropy contributions and, therefore, no dynamo for models 2 and 1, respectively. Such cooling rates would permit an inner core as old as the Earth. Higher core cooling rates generate a higher net entropy production rate; they also means that the inner core must have formed more recently.

For a present-day estimated CMB heat flow of 6–14 TW (Section 9.09.2.5), the net entropy

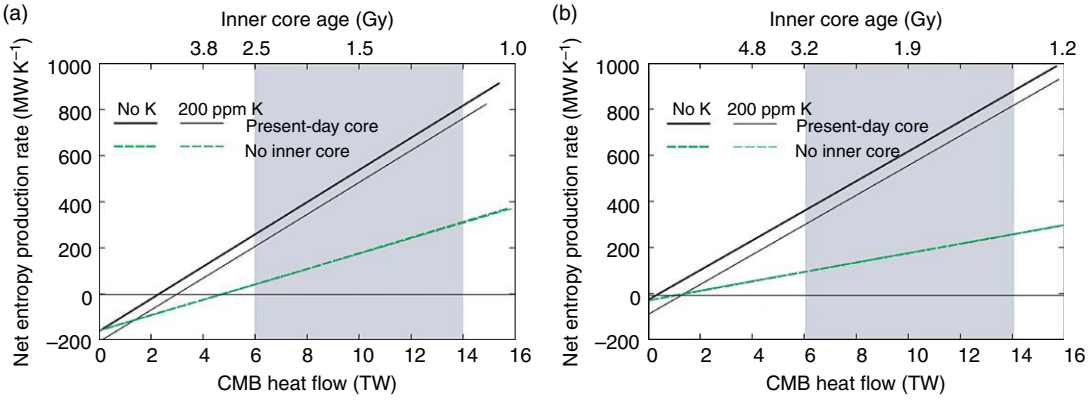

Figure 2 (a) Net entropy production (available to drive the geodynamo) as a function of CMB heat flux, for cases with and without an inner core, and with and without 200 ppm potassium. Parameters used are for model 2 in **Table 2**. Inner-core age is calculated assuming a constant core cooling rate, $\Delta T_c = 100$ K (eqn [7]) and is only relevant to the case with an inner core and no potassium. (b) As for (a), except using the parameters for model 1 in **Table 2** (designed to maximize inner-core age) with $\Delta T_c = 150$ K. The shaded region denotes the estimated present-day CMB heat flow (see Section 9.09.2.5).

production rate available to drive the dynamo is 200–900 MW K^{-1}, sufficient to generate roughly 1–5 TW of ohmic dissipation. Since most estimates of ohmic heating are less than 2 TW (Section 9.09.2.6.1), it is clear that there is no difficulty in driving a dynamo at the present day. A heat flow of 6–14 TW also implies an inner-core age of 1–2.5 Gy and 1.4–3.2 Gy for models 2 and 1, respectively, assuming a constant core cooling rate.

Prior to the formation of an inner core, the CMB heat flow had to exceed the adiabatic value Q_k in order to maintain a dynamo for reasons discussed above (eqn [12]). For a dynamo requiring an entropy production rate of 200 MW K^{-1}, the core cooling rate had to be roughly 2–3 times as fast to maintain this rate before the onset of inner-core solidification. A geodynamo prior to the onset of inner-core formation is entirely possible, but implies that either CMB heat fluxes were higher in the past, or that the present-day dynamo is dissipating more heat than it did prior to inner-core formation.

Figure 2 also shows that, as discussed above, a larger CMB heat flow is required for the same entropy production if radioactive heating is important in the present-day Earth. Prior to the existence of the inner core, the effect of radioactive decay on the entropy production is small because the thermodynamic efficiency of radioactive heat production is similar to that of secular cooling (Roberts *et al.*, 2003; Gubbins *et al.*, 2003, Chapter 8.02). Importantly, the presence of potassium also reduces the core cooling rate, and thus can increase the age of the inner core (eqn [9] and see below).

In summary, **Figure 2** shows that the estimated present-day CMB heat flow of 6–14 TW is consistent with the operation of a dynamo dissipating 1–5 TW of heat. Under these circumstances, an inner core could have persisted for 1–3.2 Gy if the heat flux stayed constant. A lower CMB heat flux would result in a lower dissipation rate and a greater inner core age. Radioactive heating can increase the inner-core age somewhat, but the present-day radioactive heat production is likely only a small fraction of the total energy budget, and thus the effects are modest. In practice, of course, both the core heat flux and the radiogenic heat production will vary with time; investigating the time evolution of the core and mantle is the subject of the next section

9.09.3.2.4 Thermal evolution

There are two basic approaches to modeling the thermal evolution of the core. One approach is to start from some assumed initial conditions and evolve the core forwards in time, using eqn [8] or its equivalent (Stevenson *et al.*, 1983; Stacey and Loper, 1984; Mollett, 1984; Yukutake, 2000; Nimmo *et al.*, 2004; Nakagawa and Tackley, 2004a, 2004b; Butler *et al.*, 2005; Costin and Butler, 2006; Davies, 2007). The initial conditions can be iterated until the correct present-day core parameters (e.g., inner-core size) are obtained, and the theoretical geodynamo history compared with the observations. Because the core's evolution depends on the CMB heat flux, such models must simultaneously track the thermal evolution of the mantle. This kind of approach has two principal disadvantages: first, it requires the assumption of initial conditions which are poorly constrained (Chapter 9.03); and second, in considering the mantle as well as the core, the number of important but uncertain parameters (e.g., mantle viscosity) greatly increases.

A second approach is to start from the present-day core conditions and evolve the core backwards in time (Buffett *et al.*, 1996; Buffett, 2002; Labrosse 2003). This approach has the advantage of automatically satisfying the present-day observations. However, because diffusion equations are unstable if run backwards in time, the evolution of the CMB heat flux cannot be calculated in the same way as it can in the forward models. A common choice is to specify the time evolution of the entropy production in the core, which then specifies both the core cooling rate and the evolution of the CMB heat flux (eqn [11]). This approach has the virtue of not requiring any knowledge of the mantle to do the calculations; however, it makes a major assumption in assuming a specific entropy production history for the core. Nonetheless, this approach is both simpler and subject to fewer uncertainties than the alternative, and will be focused on here.

Partly because of geochemical arguments that may suggest an ancient (~3.5 Gy BP) inner core (Section 9.09.3.3.1), many of the investigations cited above have focused on the age of the inner core. While there is a general tendency to find relatively young (~1 Gy) inner cores, the robustness of these results is often unclear because of the large number of poorly constrained parameters which have to be chosen. Another aim of this section is to tabulate the most important parameters, and to investigate the robustness of the thermal evolution results to likely parameter variations. In particular, we will focus on whether a 3.5 Gy old inner core is compatible with the theoretical models, and conclude that it is not, unless the core contains an additional energy source (e.g., ^{40}K).

9.09.3.2.4.(i) Parameters Generating an ancient inner core requires either a relatively low CMB heat flux, a large difference in adiabatic and melting temperature gradients, or substantial radiogenic heating. If the core cooling is slow, then to maintain the dynamo requires either low magnetic dissipation, large positive entropy terms (e.g., E_g), or small negative entropy terms (e.g., E_k).

Of the various parameters discussed in Section 9.09.2, we may identify those which will have the largest influence on whether a dynamo can be maintained while producing an ancient core. They are as follows:

1. Thermal conductivity k and thermal expansivity α. A low thermal conductivity or expansivity reduces E_k, and thus allows the same rate of entropy production for a lower CMB heat flux (eqn [11]).
2. Gradient of the melting curve. The quantity ΔT_c (eqn [7]) is the change in T_c since the inner core started solidifying, and is determined by the relative slopes of the adiabat and the melting curve. A larger ΔT_c results in an older inner core for the same CMB heat flux (or alternatively a higher entropy production rate for an inner core of the same age).
3. The compositional density contrast $\Delta\rho_c$. The larger the value of $\Delta\rho_c$, the higher the entropy production rate for the same rate of cooling.
4. The rate of entropy production required to drive the dynamo. As discussed in Section 9.09.2.6.1, this value is unlikely to be less than 50 MW K^{-1}, and is more likely closer to 200 MW K^{-1}.
5. Radioactive heating within the core. Internal heat production reduces the core cooling rate (**Figure 2** and eqn [9]).

Other factors, such as latent heat, specific heat capacity, heat of reaction and so on are either better known than the factors listed above, or have only a small effect.

Factors 1–3 are known with some uncertainty, while factors 4 and 5 are less well known. We have therefore adopted three models (**Table 2**) designed to result in maximum, best-guess, and minimum inner-core ages, respectively. In this way, a conservative assessment may be made of the model variability arising from uncertainties in parameter values.

The calculations shown below take a similar approach to those of Buffett (2002) and Labrosse (2003) and assume a specified rate of entropy production with time. The core temperature is evolved backwards from the present-day conditions. The entropy production rate prior to inner-core formation is assumed constant, which allows the CMB heat flux and core cooling rate to be determined. The CMB heat flux during inner-core solidification is assumed to stay constant at the value immediately prior to solidification. The justification for making this assumption is that the CMB heat flux is determined primarily by conditions in the mantle, and is thus unlikely to be significantly affected by changing core conditions. This assumption is less reliable for inner cores of greater ages or having larger values of ΔT_c. A result of the assumption is that the entropy production increases significantly when inner-core solidification starts, because of the extra contributions (e.g., latent heat release) to the entropy budget.

Other assumptions could be made. For instance, Labrosse (2003) assumes that the present-day entropy production is some constant factor times the entropy production immediately prior to core formation. It will be shown below that different assumptions of this kind do not significantly affect the results. In theory, one would like to use observations of the Earth's magnetic field to constrain the entropy evolution. For instance, a higher field strength should lead to greater dissipation and thus higher entropy production. Unfortunately, as discussed in Section 9.09.2.6, neither the observations, nor our theoretical understanding of geodynamos, are currently good enough to infer how the entropy production has changed. The assumption of constant entropy production prior to inner-core formation at least has the virtue of simplicity; furthermore, since if anything entropy production is likely to have declined with time, this assumption will result in conservatively old inner core ages.

Figure 3 shows the evolution of various parameters of interest for models 1–3 when the net entropy production rate prior to inner-core formation is 200 MW K^{-1}, probably a reasonable value (see Section 9.09.2.6.1). This entropy production rate determines the core cooling rate, and thus the heat flux. The present-day heat fluxes are in the range 10–15 TW, in line with expectations (Section 9.09.2.5). The change in CMB heat flow over 4 Gy is modest, a factor 25% or less. Whether such a small change is dynamically plausible is currently unclear, and will be discussed further below.

As expected, the heat flux required for model 1 is lower than for the other models, because model 1

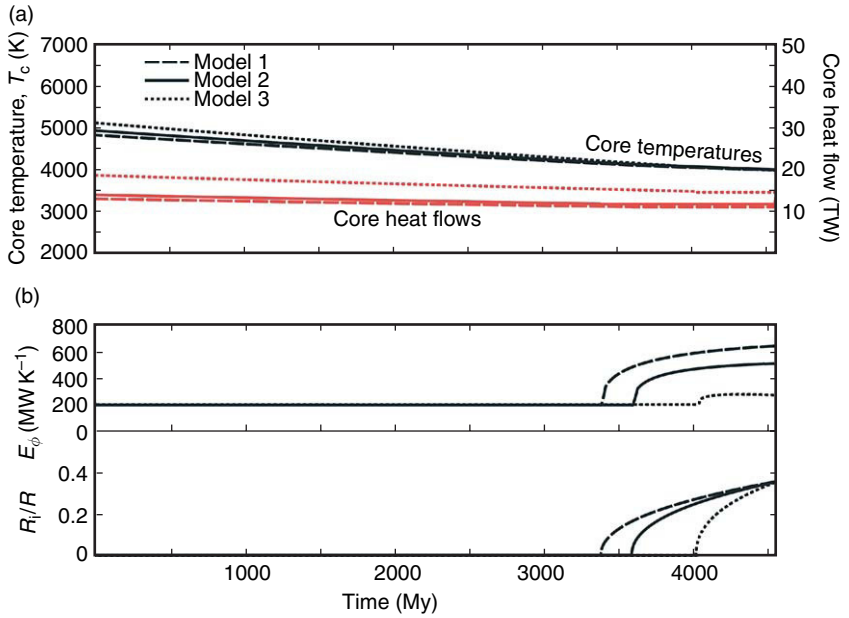

Figure 3 (a) Evolution of core heat flow and core temperature T_c with time for models 1–3 (parameter values for each model are given in **Table 2**). Heat flow prior to inner-core formation is calculated by fixing entropy production rate at 200 MW K^{-1}. Heat flow after the onset of inner-core formation is kept at the same level as it was immediately prior to solidification. Equations are integrated backwards in time from the present day. (b) Evolution of the entropy production rate E_Φ (upper panel) and dimensionless inner core radius R_i/R (lower panel) for models 1–3. Note that the entropy production increases when inner-core formation occurs.

uses parameter values chosen to favor a long-lived geodynamo. A consequence of this lower heat flux is that the temperature change of the core over 4.5 Gy is smaller than for models 2 and 3. The lower heat flux also results in an inner core of greater age, 1.2 Gy Model 1 also results in a greater amount of entropy production once core formation begins, mainly because of more vigorous compositional convection due to the large value of $\Delta\rho_c$ adopted (see **Table 2**). The total energy released since inner-core formation due to secular cooling, gravity, and latent heat is in the ratio 69:15:16 for model 1, and 61:7:32 for model 3, also illustrating the greater importance of compositional convection in model 1.

Figure 4 shows the same situation as the preceding figure, but now with a net entropy production rate prior to inner core formation of 50 MW K^{-1}, at the lower end of reasonable values. The lower entropy production results in a reduction in the heat flux required (4–12 TW at the present day), and also a reduction in the amount by which the core has cooled over 4.5 Gy. As a consequence of this reduction in cooling rate, the inner core can persist further back in time. In particular, for model 1 the age of the inner core (3.4 Gy BP) is roughly compatible with the proposed age based on Os isotope systematic (Brandon *et al.*, 2003; see Section 9.09.3.3.1).

Figure 5 is identical to **Figure 3**, but includes the effect of 200 ppm potassium in the core. The CMB heat flows required to drive the dynamo are similar to those in **Figure 3**, as expected from the results of **Figure 2**. However, the change in core temperature with time is significantly reduced, because of the additional heat source (eqn [9]). This reduction in core cooling rate also results in a more ancient inner core, though the effect is relatively modest because the radiogenic heat production is small compared to the total heat flow (cf. Labrosse 2003; Nimmo *et al.*, 2004; Butler *et al.*, 2005). At a lower entropy production rate, the effect of radioactive decay on the inner core age would be more pronounced.

9.09.3.2.5 *Inner-core age*

Figure 6 summarizes the outcomes of several similar models by plotting inner-core age (i.e., the age of the onset of crystallization) against present-day CMB heat flux, for cases with and without potassium. As expected, a higher Q_{cmb} results in a younger inner core. For the same heat flux, model 1 results in an

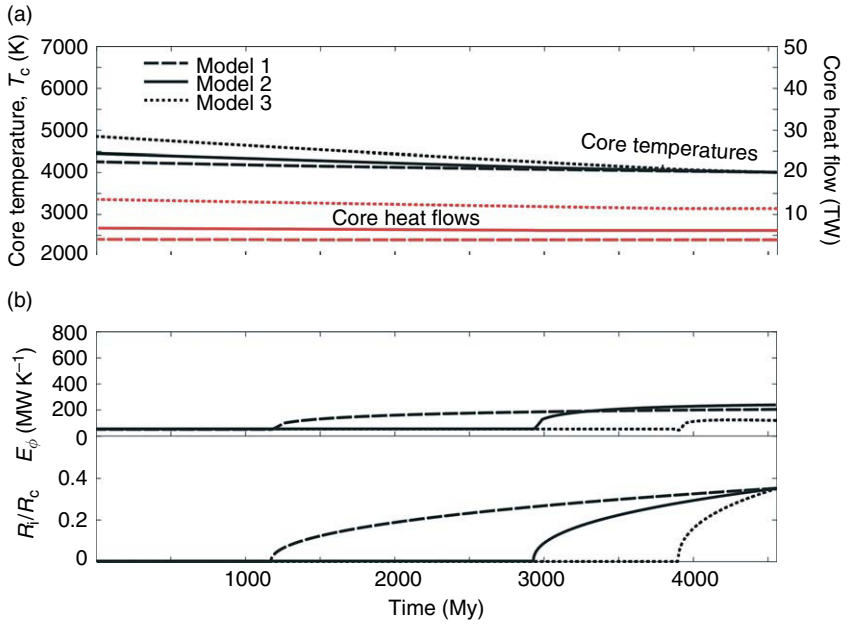

Figure 4 As for **Figure 3**, but with the net entropy production rate prior to inner-core formation fixed at 50 MW K^{-1}.

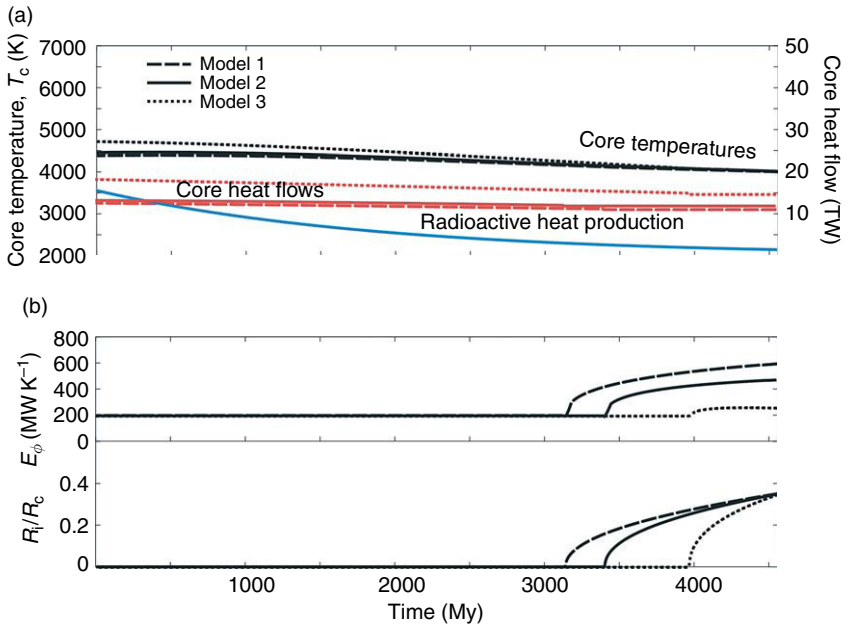

Figure 5 As for **Figure 3**, but with the core containing 200 ppm potassium. The rate of heat production within the core is shown.

older inner core than models 2 and 3, and also generates a higher rate of entropy production.

In the absence of potassium, **Figure 6(a)** shows that an inner core 3.5 Gy old is possible. However, for the inner core to be this old, the following requirements must all be met:

1. Parameters such as thermal conductivity, expansivity, and compositional density contrast must all have values (**Table 2**) which tend to maximize the inner core age.
2. The rate of entropy production required to drive the dynamo is small, <50 MW K^{-1}. In terms of

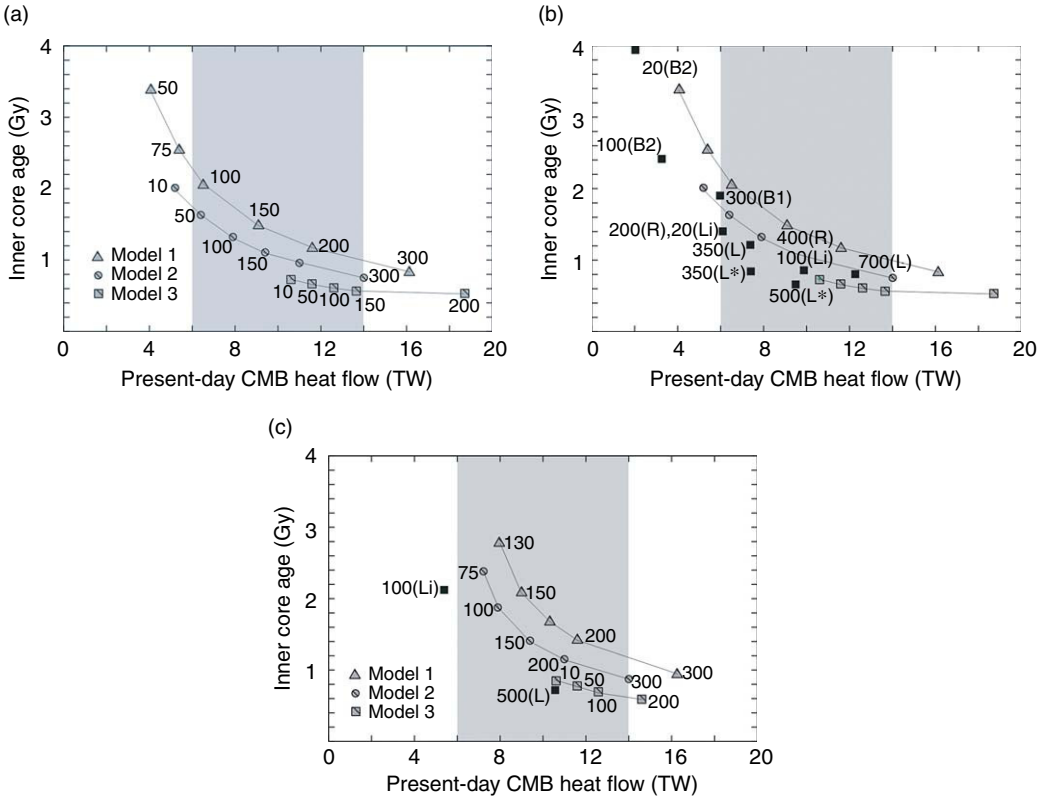

Figure 6 (a) Plot of present-day CMB heat flux against inner-core age, from a suite of models similar to those shown in **Figures 3** and **4**. The labels refer to the constant entropy production rate (in MW K^{-1}) prior to the onset of inner core formation. Higher entropy production rates require higher heat fluxes and thus younger inner cores. (b) Same plot as (a), but showing results obtained by other authors. As before, labels indicate entropy production rate; parentheses give references as follows: B2 = Buffett (2002); B1 = Buffett *et al.* (1996); R = Roberts *et al.* (2003); L and L* = Labrosse (2003); Li = Lister (2003). The latter two models have entropy production rates prior to inner-core formation which are not quite constant. Ohmic dissipation is converted to entropy production by assuming a characteristic temperature of 5000 K. (c) As for (a), but with 200 ppm potassium in the core. The black squares are results from Labrosse (2003) and Lister (2003) with 250 and 235 ppm potassium in the core, respectively.

dissipation, this is ≈0.25 TW, at the low end of current estimates (Section 9.09.2.6.1).

3. The CMB heat flux must have stayed low and relatively constant, with a mean value of about 4 TW over the whole of Earth history (cf. **Figure 4**).

Requirements 1 and 2 are at least possible, if not plausible. Requirement 3 is, however, more problematic. First, the required heat flux is a factor of 1.5–4 times smaller than the inferred present-day CMB heat flux of 6–14 TW (Section 9.09.2.5). An inner core 3.5 Gy old is incompatible with current estimates of the present-day CMB heat flux, unless D″ contains significant quantities of radiogenic materials (Section 9.09.2.5; see also Buffett (2002) and Costin and Butler (2006)).

The requirement that the CMB heat flux stay essentially constant over time is surprising, because the reduction in core temperature with time is likely to lead to an increase in mantle viscosity and a decrease in CMB heat flux (Nimmo *et al.*, 2004). However, whether a constant CMB heat flux is dynamically plausible is unclear (e.g., Davies, 2007), because our understanding of the physical nature of the CMB region is currently so poor (Section 9.09.2.5).

Figure 6(b) compares the results obtained here with those obtained by other authors. Despite the different assumptions and parameters chosen, the results are strikingly consistent. In general, the results plot between the lines for models 2 and 3, suggesting that model 1 is overly conservative (as it was designed to be). Models using a present-day heat flux of 6–14 TW result in entropy production rates of 200–700 MW K^{-1}, which are perfectly reasonable values, and an inner-core age range of 0.6–2 Gy. Conversely, to achieve an ancient inner core requires

both low entropy production and low CMB heat fluxes (e.g., 20 MW K^{-1} and 2 TW from Buffett (2002)).

As has been recognized previously (Buffett, 2002; Labrosse, 2003; Roberts *et al.*, 2003; Nimmo *et al.*, 2004), the difficulty of generating an ancient inner core while maintaining a dynamo is reduced if the core contains a radioactive heat source such as potassium. With 200 ppm in the core, **Figure 6** shows that an inner core 3 Gy old is compatible with a reasonable present-day heat flux (8 TW) and an entropy production rate of 130 MW K^{-1}, likely sufficient to sustain a geodynamo. Thus, the addition of potassium makes it much easier to reconcile the geophysical models with an ancient inner core.

9.09.3.2.6 Initial core temperature

An issue closely related to the age of the inner core is the initial core temperature. Here 'initial' refers not to the temperature of the core during accretion (which may have been as high as 10 000 K – *see* Chapter 9.03), but to the temperature once accretion had finished and the density structure of the Earth resembled the present-day arrangement. Higher rates of entropy production imply younger inner cores and more rapid core cooling, which in turn implies a higher initial core temperature (Buffett, 2002; Labrosse, 2003). **Figure 7** plots the variation in initial core temperature as a function of entropy production for models 1–3, and demonstrates the relationship. **Figure 7(b)** includes the effect of 200 ppm potassium, demonstrating that internal heat production reduces the required change in core temperature (eqns [9] and [10]). These figures also demonstrate how inner-core age (labels on individual points) is increased by either a lower entropy production rate, or the addition of potassium. In extreme cases, the inner core could have been present for the entire age of the Earth.

The results shown here are again consistent with those of other authors. One result from Buffett (2002) is plotted and again shows that ancient inner cores require low dissipation rates, and imply cool initial temperatures. Labrosse (2003) assumes higher-entropy production rates (350–700 MW K^{-1}) and obtains correspondingly younger inner cores (0.8–1.2 Gy) and hotter initial temperatures (roughly 600 K hotter than the present day).

The most striking aspect of **Figure 7** is that a core temperature change of less than 1000 K ($T_c < 5000$ K at $t = 0$) is sufficient to have maintained a moderately dissipative dynamo ($E_\phi < 200$ MW K^{-1}) throughout Earth history. This is in contrast to the results presented in Chapter 9.03, which inferred an initial core temperature of 5500 K or more. While the latter estimate in particular is somewhat crude, the discrepancy in the two estimates is interesting because of the additional insight it may provide.

The discrepancy could be resolved in at least two ways. First, the geodynamo could be more dissipative than assumed, either now or in the past. Future palaeomagnetic measurements might be able to confirm or disprove this possibility. Second, the core temperatures shown in **Figure 7** are sufficiently

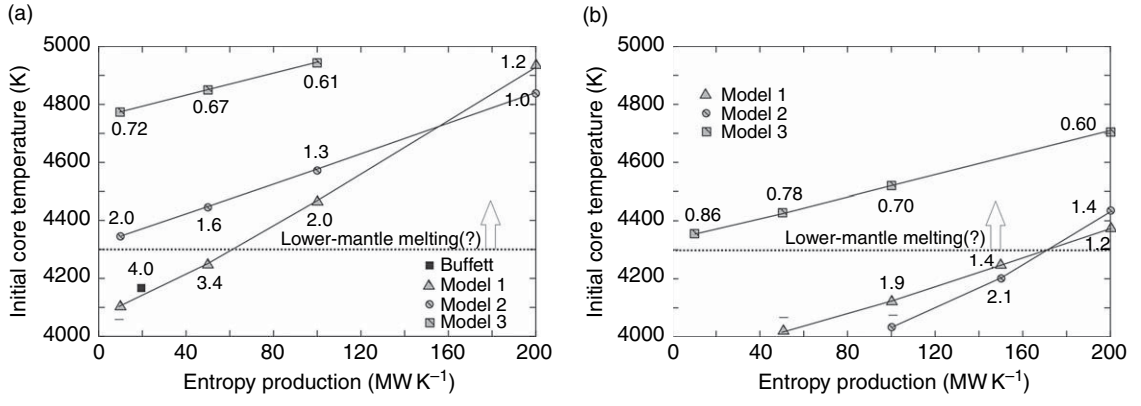

Figure 7 (a) Variation in initial-core temperature with (constant) entropy production rate prior to core formation, obtained from a suite of models similar to those shown in **Figures 3** and **4**. Labels indicate inner-core age in Gy; higher entropy production rates require more rapid core cooling and thus high initial temperatures and young inner cores. The black square represents a result from Buffett (2002) with low entropy production and a correspondingly ancient inner core; here the temperature change (160 K) obtained is plotted assuming a present-day temperature of 4000 K. Horizontal dotted line indicates onset of mantle melting (Boehler, 2000) and is uncertain by at least ±200 K.

high that the early mantle was likely extensively molten. The melting behavior of the lowermost mantle is poorly known (Boehler, 2000; Akins *et al.*, 2004), especially for the postperovskite phase. Nonetheless, it seems likely that the CMB heat flux would have been elevated if the early lower mantle were extensively molten. Thus, the CMB heat flux probably consisted of two periods: an early, high heat flux episode due to the molten lower mantle; and later, lower heat fluxes resembling the trajectories shown in **Figures 3–5**.

The early episode of high heat flux will have persisted until the lower mantle approached its solidus, so the core likely cooled by several thousand kelvins over this period. The heat capacity of the core is roughly $2 \times 10^{27}\,\mathrm{J\,K^{-1}}$; thus, if the period lasted 1 Gy, the mean heat flow must have been of order 100 TW. How such large heat fluxes could have been sustained by the mantle is very much an open question. The high heat fluxes required also illustrate the difficulty of forming an early inner core, if the initial core temperatures were as high as estimated in Chapter 9.03. Finally, the high initial heat fluxes imply a potentially very strong early magnetic field; palaeointensity measurements from rocks or minerals (e.g., zircons) of the appropriate age would thus be an excellent test of this hypothesis.

9.09.3.2.7 Consequences for the mantle

The above discussion illustrates an important point: the thermal evolution of the core cannot really be considered separately from the thermal evolution of the mantle. In particular, the evolution of the CMB heat flux controls the thermal evolution of the core, and yet is to a large extent determined by mantle processes. Conversely, the early state of the core implies that the lowermost mantle was probably extensively molten, with potentially important consequences for mantle chemistry and dynamics.

Although the need to also consider the mantle increases the number of free parameters in theoretical models, it also adds potential extra observational constraints. For instance, the evolution of the mantle temperature depends on three factors: internal heat generation; heat added from the core; and the rate of heat loss to the surface. Some petrological constraints on the evolution of mantle temperatures exist (e.g., Abbott *et al.*, 1994; Grove and Parman, 2004). Unfortunately, in order to provide constraints on the evolution of the CMB heat flux, the manner in which the surface heat flux varied with time must be known. This heat flux is controlled at the present day by plate tectonics, but how it varied in the past (and indeed, whether plate tectonics actually operated) is currently unknown. Thus, the addition of extra information (evolution of mantle temperatures) is offset by the addition of additional uncertainties (evolution of surface heat flux).

9.09.3.3 Compositional Evolution

The compositional evolution of the core since its formation has been a relatively neglected field of study, perhaps because of the paucity of observational constraints. There are two main ways in which the core composition evolves: through solidification of the inner core; and through reaction with the mantle at the CMB. Each of these is dealt with briefly in turn; a good review of some of the consequences of inner-core growth may be found in Sumita and Yoshida (2003).

9.09.3.3.1 Inner-core growth

One potentially observable consequence of inner-core growth is its effect on Os isotope systematics. The basic hypothesis is relatively simple (Walker *et al.*, 1995): both Re and Pt are presumed to partition preferentially into the outer core relative to Os as solidification proceeds. Since ^{187}Re and ^{190}Pt decay to ^{187}Os and ^{186}Os, respectively, the outer core will become progressively enriched in these Os isotopes relative to stable ^{188}Os. The amount of enrichment depends on the time since inner core crystallization, and the relative partitioning of Re and Pt into the outer core compared to Os. Furthermore, the enrichments in ^{186}Os and ^{187}Os are expected to be coupled if core crystallization occurs (since both are occurring due to the same process).

There are two sets of observations (Brandon *et al.*, 1998, 2003). First, ancient (2.7–2.8 Ga) komatiites show evidence of elevated and coupled Os-isotope ratios, which could be indicative of early core solidification. Second, more recently erupted lavas in Hawaii, Siberia, and Gorgona Island all show elevated and coupled Os-isotope ratios, again consistent with an outer-core source. Assuming values for the partition coefficients of Pt, Re, and Os, it has been argued (Brandon *et al.*, 2003) that the onset of inner-core crystallization must have been prior to 3.5 Ga to explain the komatiite Os-isotope ratios.

There are several possible objections to this hypothesis. The first is simply that the partition coefficients at the correct P, T conditions are

currently uncertain. Since the evolution of the Os-isotope ratios depends on the partition coefficients, all that the komatiite data can really be used to argue is that inner-core crystallization began at least a few hundred million years prior to 2.7–2.8 Ga (Puchtel *et al.*, 2005), assuming that the isotopic signal is in fact due to crystallization. Although partition coefficients for Pt, Re, and Os have been measured (at 10 GPa and 1700 K; Walker (2000)), and also inferred from meteorites (Morgan *et al.*, 1995), the behavior is likely to be different at higher P, T conditions. Initial experiments at pressures up to 22 GPa in an Fe–S system suggest partition coefficients that are too low to explain the Os-isotopic observations (Van Orman, personal communication).

More seriously, it is not clear that the Os-isotopic signals can only be explained by inner-core crystallization. In particular, it has been suggested that recycled oceanic crust and/or sediments could equally explain the coupled signals (Hauri and Hart, 1993; Baker and Jensen, 2004; Schersten *et al.*, 2004), though that conclusion has been disputed (Brandon *et al.*, 2003; Puchtel *et al.*, 2005). The absence of detectable tungsten (Schersten *et al.*, 2004) and lead (Lassiter, 2006) isotope anomalies in Hawaiian lavas has been used to argue against the presence of any core materials. However, it is possible that these signals have been masked by contributions from recycled crust (Brandon and Walker, 2005). Recently, both Fe/Mn ratios (Humayun *et al.*, 2004) and thallium isotopes (Nielsen *et al.*, 2006) have been used to argue against crust or sediments as the source of the Os-isotope anomalies.

There is thus currently little agreement on whether or not Os isotopes can tell us anything about the crystallization of the inner core (see Brandon and Walker (2005) and Lassiter (2006) for recent – and opposed – reviews). A major step forward would be to determine the relevant partition coefficients under the P, T conditions appropriate to the inner core (5000 K, 300 GPa). Doing so experimentally is challenging, in which case molecular dynamics simulations may be the correct approach. Resolving this issue is a key question since thermal evolution models tend to result in a wide range of inner-core ages (Section 9.09.3.2.5).

Another consequence of inner-core growth is that it involves the expulsion of one or more light elements into the outer core. Unless, as is commonly assumed, they are efficiently mixed into the outer core by convective stirring, these elements will rise to the CMB and generate a stably stratified layer (see Braginsky (2006) and references therein). A similar situation may arise if the heat flux out of the top of the core is subadiabatic (Labrosse *et al.*, 1997; Lister and Buffett, 1998). If it exists, such a layer will have important consequences for heat transfer across the CMB, and the temperature structure of the core. Some evidence has been adduced for the presence of this layer based on observations of the Earth's varying rotation and magnetic field (Braginsky, 1993; Lister and Buffett, 1998). Unfortunately, the ~100 km layer thickness suggested by these observations is unlikely to be detectable by seismological observations, and thus its presence remains somewhat hypothetical.

Rather than the light elements segregating to form a separate layer, it has instead been argued (Buffett *et al.*, 2000) that the addition of elements (specifically Si and O) to the outer core drives a chemical reaction, resulting in a silicate-rich layer of light sediments at the top of the core. These silicates will ultimately be incorporated into the mantle and will contain a few percent residual iron. Thus, this mechanism is one way of incorporating core material into the mantle, in possible agreement with the Re–Os–Pt observations. A similar outcome is proposed by Dubrovinsky *et al.* (2004), who argue that the decreasing solubility of Si in iron with increasing pressure means that Si incorporated into core material within the magma ocean will be expelled as core pressures rise, and accumulate at the top of the core.

9.09.3.3.2 Core–mantle boundary

There is undoubtedly a region at the CMB over which core and mantle materials have reacted (Knittle and Jeanloz, 1991). However, neither the vertical extent of this region, nor the manner in which it has evolved with time, are well understood. Observations based on Earth nutations suggest that the CMB region must include a thin, relatively conductive layer (e.g., Buffett *et al.*, 2002). Poirier *et al.* (1998), however, concluded that capillarity driven infiltration of the mantle by fluid iron is only likely to extend for tens of meters, though effects such as mantle deviatoric stresses may extend this range to ~1 km (Kanda and Stevenson, 2006). Thicker, iron-rich layers can strongly affect mantle dynamics (Manga and Jeanloz, 1996) and may be swept up into the mantle (Sleep, 1988; Kellogg and King, 1993). However, downwards drainage of liquid iron will be orders of magnitude more rapid than the rate

at which it can be swept up (Poirier *et al.*, 1998). Furthermore, if the thickness of the iron-rich layer is much smaller than the convective boundary-layer thickness, the rate of entrainment will be negligible. Thus, on physical grounds, it seems difficult for core or CMB material to be transported to the near surface, although as discussed above there are isotopic arguments that it may have occurred.

9.09.3.4 Summary

Neither the thermal nor the compositional evolution of the core are currently very well understood, because of a lack of observational data (Section 9.09.2.6) and considerable uncertainties in the relevant parameter values. Nonetheless, by assuming that ohmic dissipation was constant prior to inner-core formation, and by using models spanning the likely range of parameter values, the thermal history of the core can be investigated, with results summarized in **Figures 6** and **7**. Several important points are evident.

First, there is no difficulty in maintaining a moderately dissipative dynamo prior to inner-core formation as long as the core is cooling fast enough (cf. **Figures 2–5**); an inner core is not required to drive the early geodynamo.

Second, a higher CMB heat flux implies a more dissipative dynamo and a younger inner core, although the addition of potassium can make the inner core somewhat older (**Figure 6**). An estimated present-day CMB heat flux of 6–14 TW is consistent with a constant entropy production rate of 50–300 MW K^{-1} and an inner-core age of 0.8–1.6 Gy, assuming best-guess core parameters (model 2).

Third, a 3.5 Gy old inner core is possible in the absence of radiogenic heating, but only if the ohmic dissipation is <0.25 TW and the CMB heat flow has stayed constant at 4 TW. The addition of 200 ppm potassium allows an inner core to persist over the whole of Earth history for heat flows less than about 8 TW (**Figure 6(c)**). If the Os-isotope data indicating a 3.5 Gy old inner core are correct (Section 9.09.3.3.1), the implications for the thermal history of the core are profound, since they require either low CMB heat flow and low ohmic dissipation, or significant amounts of potassium in the core. However, it is currently far from clear that the Os-isotope signals are actually derived from core material.

Fourth, a moderately dissipative dynamo operating for 4 Gy implies initial core temperatures 200–800 K hotter than the present day, or somewhat less if potassium is present (**Figure 7**). These temperatures imply that the early lower mantle was probably extensively molten, with very uncertain consequences for the CMB heat flux. It is also notable that the initial temperatures shown in **Figure 7** are significantly smaller than the values calculated by Chapter 9.03, based on gravitational potential energy release. This discrepancy is likely the result of either a significantly more dissipative core or, more probably, an early period of rapid core cooling as a result of the molten lower mantle.

There are several ways in which future progress in the study of the long-term evolution of the core is likely to be made:

1. A major step toward resolving the issue of whether the Os-isotope data provide information on inner-core formation would be the measurement of partition coefficients at the relevant P, T conditions. At least for a potassium-free core, an inner core 3.5 Gy old requires a thermal evolution that is at odds with a continuous geodynamo and geophysical expectations of the CMB heat flux. Resolving whether or not the Os data really constrain the inner-core age is thus of great importance.
2. The likelihood that the lower mantle was initially extensively molten has consequences for the chemical and particularly thermal evolution of the mantle which are not understood. In particular, if lower-mantle melts are indeed denser than the solid (e.g., Knittle, 1998; Akins *et al.*, 2004), it is not even clear that heat transfer will be enhanced.
3. More generally, the evolution of the CMB heat flux is not well constrained, while being absolutely central to the evolution of the core and geodynamo (cf. Nimmo *et al.*, 2004; Davies, 2007). Complicating factors such as possible melting, the postperovskite phase transition, and perhaps chemical layering, render dynamical models uncertain. The models shown in **Figures 3–5** (which do not include any dynamics) suggest a CMB heat flux which does not vary greatly over 4 Gy; it is not yet clear whether such results are dynamically plausible. So far, few models have included the available observational constraints on mantle cooling rates, which may help to reduce the possible parameter space (Section 9.09.3.2.7).
4. Whether or not the core contains any potassium is still an unresolved issue. If the Os-isotope inference of an ancient inner core is correct, then the

presence of potassium makes it much easier to reconcile the geophysical models with the inner-core age (Section 9.09.3.2.5 and **Figure 6**). Conversely, if the core lacks potassium, an ancient inner core becomes much more difficult to explain (Lassiter, 2006). At present, the best constraints on core potassium abundance are likely to come by comparing potassium concentrations with those of other elements with similar affinities for iron.

5. Although uncertainties in many of the relevant parameters have been reduced (Section 9.09.2), there are still gaps. In particular, the core thermal conductivity is a key parameter which is poorly known; further experiments to confirm the important work of Bi *et al.* (2002) are sorely needed.
6. Finally, one would expect the changing CMB heat flux and the growth of the inner core to have observable effects on the behavior of the geodynamo. Thus, at least in principle, the palaeomagnetic record ought to provide observational constraints on core thermal evolution. For instance, the presence of an inner core appears to have an effect on the time variability of the magnetic field (Roberts and Glatzmaier, 2001); thus, good enough palaeomagnetic data may help to tie down when the inner core formed (Coe and Glatzmaier, 2006).

9.09.4 Conclusions

This chapter set out to examine the thermal and compositional evolution of the core, from shortly after its formation to the present day. This period probably involved only two events of importance: the initiation of the geodynamo and the onset of inner-core formation. Geodynamo activity started at 3.5 Gy BP at the latest; however, it is important to understand that this dynamo could easily have been sustained without an inner core being present. Theoretical estimates suggest that the inner core probably formed at ~1 Gy BP, unless either significant quantities of potassium were present in the core, or both the ohmic dissipation (<0.25 TW) and the CMB heat flow (<4 TW) were very low (**Figure 6**). The Re–Os–Pt isotopic system has been used to infer that inner-core solidification started by 3.5 Gy BP, but this hypothesis remains highly controversial.

Assuming a moderately dissipative dynamo, the change in core temperature over 4 Gy was probably 200–800 K, implying an early lower mantle that was likely extensively molten. These initial temperatures are lower than those obtained by consideration of the gravitational potential energy release during core formation, and suggest that the CMB heat flux evolved in two stages: an early, high heat flux stage, presumably due to the melting of the lower mantle, and potentially generating very strong magnetic fields; and a later, lower heat flux stage resembling the results shown in **Figures 3–5**.

The present-day core geodynamo is maintained primarily by compositional convection as the inner core solidifies. The CMB heat flux is estimated at 10 ± 4 TW and is sufficient to drive a dynamo dissipating 1–5 TW.

As should be clear, there are several areas which require further study. First, there is still a discrepancy between estimates of the inner-core age based on isotopic systematics and those based on geophysical models. Second, neither cosmochemical nor geophysical arguments have so far provided a convincing resolution to the debate over whether the core contains significant potassium. Third, the evolution of the CMB heat flux over time is currently poorly understood, particularly the effect of lower-mantle melting, and yet has first-order implications for the thermal history of both core and mantle. Fourth, estimates of material properties, especially core conductivity, at the correct conditions need to be more accurate. Finally, future palaeomagnetic measurements may help to provide further observational constraints on the evolution of the geodynamo, and thus the thermal evolution of the core.

Acknowledgment

This work is supported by NSF-EAR.

References

Abbott D, Burgess L, Longhi J, and Smith WHF (1994) An empirical thermal history of the Earth's upper mantle. *Journal of Geophysical Research* 99: 13835–13850.

Abe Y, Ohtani E, Okuchi T, Righter K, and Drake M (2000) Water in the early Earth. In: Canup RM and Righter K (eds.) *Origin of the Earth and Moon*, pp. 413–434. Tucson, AZ: University of Arizona Press.

Adler JF and Williams Q (2005) A high-pressure X-ray diffraction study of iron nitrides: Implications for Earth's core. *Journal of Geophysical Research* 110: B01203.

Akins JA, Luo S-N, Asimow PD, and Ahrens TJ (2004) Shock-induced melting of $MgSiO_3$ perovskite and implications for melts in Earth's lowermost mantle. *Geophysical Research Letters* 31: L14612.

Alfè D, Gillan MJ, and Price GD (1999) The melting curve of iron at the pressures of the Earth's core from *ab initio* calculations. *Nature* 401: 462–464.

Alfè D, Gillan MJ, and Price GD (2002a) *Ab initio* chemical potentials of solid and liquid solutions and the chemistry of the Earth's core. *Journal of Chemical Physics* 116: 7127–7136.

Alfè D, Price GD, and Gillan MJ (2002b) Iron under Earth's core conditions: Liquid-state thermodynamics and high-pressure melting curve from *ab initio* calculations. *Physical Review B* 65: 165118.

Alfè D, Gillan MJ, and Price GD (2003) Thermodynamics from first principles: Temperature and composition of the Earth's core. *Minerological Magazine* 67: 113–123.

Alfè D, Price GD, and Gillan MJ (2004) The melting curve of iron from quantum mechanics calculations. *Journal of Physics and Chemistry of Solids* 65: 1573–1580.

Allegre CJ, Manhes G, and Gopel C (1995b) The age of the Earth. *Geochemica et Cosmochimica Acta* 59: 1445–1456.

Allegre CJ, Poirier J-P, Humler E, and Hofmann AW (1995a) The chemical composition of the Earth. *Earth and Planetary Science Letters* 134: 515–526.

Anderson OL (1998) The Gruneisen parameter for iron at outer core conditions and the resulting conductive heat and power in the core. *Physics of the Earth and Planetary Interiors* 109: 179–197.

Araki T, Enomoto S, Furuno K, *et al.* (2005) Experimental investigation of geologically produced antineutrinos with KamLAND. *Nature* 436: 499–503.

Backus GE (1975) Gross thermodynamics of heat engines in deep interior of Earth. *Proceedings of the National Academy of Sciences USA* 72: 1555–1558.

Baker JA and Jensen KK (2004) Coupled Os-186-Os-187 enrichements in the Earth's mantle – core–mantle interaction or recycling of ferromanganese crusts and nodules? *Earth and Planetary Science Letters* 220: 277–286.

Belonoshko AB, Ahuja R, and Johansson B (2000) Quasi - *Ab initio* molecular dynamic study of Fe melting. *Physical Review Letters* 84: 3638–3641.

Bi Y, Tan H, and Jin F (2002) Electrical conductivity of iron under shock compression up to 200 GPa. *Journal of Physics: Condensed Matter* 14: 10849–10854.

Bloxham J (2000) Sensitivity of the geomagnetic axial dipole to thermal core–mantle interactions. *Nature* 405: 63–65.

Boehler R (1993) Temperatures in the Earth's core from melting-point measurements of iron at high static pressures. *Nature* 363: 534–536.

Boehler R (2000) High-pressure experiments and the phase diagram of lower mantle and core materials. *Reviews of Geophysics* 38: 221–245.

Boyet M and Carlson RW (2005) Nd-142 evidence for early (>4.53 Ga) global differentiation of the silicate Earth. *Science* 309: 576–581.

Braginsky SI (1963) Structure of the F layer and reasons for convection in the Earth's core. *Doklady Akademii Nauk SSSR English Translation* 149: 1311–1314.

Braginsky SI (1993) MAC-oscillations of the hidden ocean of the core. *Journal of Geomagnetism and Geoelectricity* 45: 1517–1538.

Braginsky SI (2006) Formation of the stratified ocean of the core. *Earth and Planetary Science Letters* 243: 650–656.

Braginsky SI and Roberts PH (1995) Equations governing convection in Earth's core and the geodynamo. *Geophysical and Astrophysical Fluid Dynamics* 79: 1–97.

Brandon A and Walker RJ (2005) The debate over core–mantle interaction. *Earth and Planetary Science Letters* 232: 211–225.

Brandon AD, Walker RJ, Morgan JW, Norman MD, and Prichard HM (1998) Coupled Os-186 and Os-187 evidence for core–mantle interaction. *Science* 280: 1570–1573.

Brandon AD, Walker RJ, Puchtel IS, Becker H, Humayun M, and Revillon S (2003) Os-186-Os-187 systematics of Gorgona Island komatiites: Implications for early growth of the inner core. *Earth and Planetary Science Letters* 206: 411–426.

Brown JM and McQueen RG (1986) Phase-transitions, Gruneisen parameter and elasticity for shocked iron between 77 GPa and 400 GPa. *Journal of Geophysical Research* 91: 7485–7494.

Buffett BA (2002) Estimates of heat flow in the deep mantle based on the power requirements for the geodynamo. *Geophysical Research Letters* 29: 1566.

Buffett BA (2003) The thermal state of Earth's core. *Science* 299: 1675–1677.

Buffett BA, Garnero EJ, and Jeanloz R (2000) Sediments at the top of the Earth's core. *Science* 290: 1338–1342.

Buffett BA, Huppert HE, Lister JR, and Woods AW (1996) On the thermal evolution of the Earth's core. *Journal of Geophysical Research* 101: 7989–8006.

Buffett BA, Matthews PM, and Herring TA (2002) Modeling of nutation and precession: Effects of electromagnetic coupling. *Journal of Geophysical Research* 107: 2070.

Bukowinski MST and Akber-Knutson S (2005) The role of theoretical mineral physics in modeling the Earth's interior. In: Van der Hilst RD, Bass JD, Matas J, and Trampert J (eds.) *Geophysical Monograph 160: Earth's Deep Mantle: Structure, Composition and Evolution*, pp. 165–186. Washington, DC: American Geophysical Union.

Bullard EC (1950) The transfer of heat from the core of the Earth. *Monthly Notices of the Royal Astronomical Society* 6: 36–41.

Bunge HP (2005) Low plume excess temperature and high core heat flux inferred from non-adiabatic geotherms in internally-heated mantle circulation models. *Physics of the Earth and Planetary Interiors* 153: 3–10.

Butler SL, Peltier WR, and Costin SO (2005) Numerical models of the Earth's thermal history: Effects of inner-core solidification and core potassium. *Physics of the Earth and Planetary Interiors* 152: 22–42.

Busse FH (2000) Homogeneous dynamos in planetary cores and in the laboratory. *Annual Review of Fluid Mechanics* 32: 383–408.

Cao AM and Romanowicz B (2004) Constraints on density and shear velocity contrasts at the inner core boundary. *Geophysical Journal International* 157: 1146–1151.

Carlson RW and Hauri EH (2001) Extending the Pd-107-Ag-107 chronometer to low Pd/Ag meteorites with multicollector plasma-ionization mass spectrometry. *Geochemica et Cosmochimica Acta* 65: 1839–1848.

Chambers JE (2003) Planet formation. In: Davis AM (ed.) *Treatise on Geochemistry, vol. 1: Meteorites, Comets, and Planets*, pp. 461–475. Amsterdam: Elsevier.

Christensen UR and Olson P (2003) Secular variation in numerical geodynamo models with lateral variations of boundary heat flow. *Physics of the Earth and Planetary Interiors* 138: 39–54.

Christensen UR and Tilgner A (2004) Power requirements of the geodynamo from Ohmic losses in numerical and laboratory dynamos. *Nature* 429: 169–171.

Coe RS and Glatzmaier GA (2006) Symmetry and stability of the geomagnetic field. *Geophysical Research Letters* 33: L21311.

Coltice N and Ricard Y (1999) Geochemical observations and one layer mantle convection. *Earth and Planetary Science Letters* 174: 125–137.

Costin SO and Butler SL (2006) Modelling the effects of internal heating in the core and lowermost mantle on the Earth's magnetic history. *Physics of the Earth and Planetary Interiors* 157: 55–71.

Davies GF (1988) Ocean bathymetry and mantle convection. Part 1: Large-scale flow and hotspots. *Journal of Geophysical Research* 93: 10467–10480.

Davies GF (2007) Mantle regulation of core cooling: A geodynamo without core radioactivity? *Physics of the Earth and Planetary Interiors* 160: 215–229.

Dubrovinsky L, Dubrovisky L, Langenhorst F, *et al.* (2004) Reaction of iron and silica at core–mantle boundary conditions. *Physics of the Earth and Planetary Interiors* 146: 243–247.

Dunlop DJ and Yu Y (2004) Intensity and polarity of the geomagnetic field during Pre-cambrian time. In: Channell JET, Kent DV, Lowrie W, and Meert JG (eds.) *Geophysical Monograph 145: Timescales of the Paleomagnetic Field*, pp. 85–110. Washington, DC: American Geophysical Union.

Garnero EJ, Revenaugh J, Williams Q, Lay T, and Kellogg LH (1998) Ultralow velocity zone at the core–mantle boundary. In: Gurnis M, Wysession ME, Knittle E, and Buffet BA (eds.) *Geodynamic Series 28: The Core–Mantle Boundary Region*, pp. 319–334. Washington, DC: American Geophysical Union.

Gessman CK and Wood BJ (2002) Potassium in the Earth's core? *Earth and Planetary Science Letters* 200: 63–78.

Glatzmaier GA (2002) Geodynamo simulations – How realistic are they? *Annual Review of Earth and Planetary Science* 30: 237–257.

Glatzmaier GA, Coe RS, Hongre L, and Roberts PH (1999) The role of the Earth's mantle in controlling the frequency of geomagnetic reversals. *Nature* 401: 885–890.

Glatzmaier GA and Roberts PH (1996) An anelastic evolutionary geodynamo simulation driven by compositional and thermal convection. *Physica D* 97: 81–94.

Grove TL and Parman SW (2004) Thermal evolution of the Earth as recorded by komatiites. *Earth and Planetary Science Letters* 219: 173–187.

Gubbins D (1977) Energetics of the Earth's core. *Journal of Geophysics* 43: 453–464.

Gubbins D, Alfe D, Masters G, Price GD, and Gillan MJ (2003) Can the Earth's dynamo run on heat alone? *Geophysical Journal International* 155: 609–622.

Gubbins D, Alfe D, Masters G, Price GD, and Gillan MJ (2004) Gross thermodynamics of two-component core convection. *Geophysical Journal International* 157: 1407–1414.

Gubbins D, Masters TG, and Jacobs JA (1979) Thermal evolution of the Earth's core. *Geophysical Journal of the Royal Astronomical Society* 59: 57–99.

Hage H and Muller G (1979) Changes in dimensions, stresses and gravitational energy of the Earth due to crystallization at the inner core boundary under isochemical conditions. *Geophysical Journal of the Royal Astronomical Society* 58: 495–508.

Halliday AN (2004) Mixing, volatile loss and compositional change during impact-driven accretion of the Earth. *Nature* 427: 505–509.

Harper CL and Jacobsen SB (1996) Evidence for Hf-182 in the early solar system and constraints on the timescale of terrestrial accretion and core formation. *Geochemica et Cosmochimica Acta* 60: 1131–1153.

Hauri EH and Hart SR (1993) Re–Os isotope systematics of HIMU and EMII oceanic island basalts from the South Pacific ocean. *Earth and Planetary Science Letters* 114: 353–371.

Helffrich G and Kaneshima S (2004) Seismological constraints on core composition from Fe–O liquid immiscibility. *Science* 306: 2239–2242.

Hernlund JW, Thomas C, and Tackley PJ (2005) A doubling of the post-perovskite phase boundary and structure of the Earth's lowermost mantle. *Nature* 434: 882–886.

Hewitt J, McKenzie DP, and Weiss NO (1975) Dissipative heating in convective flow. *Journal of Fluid Mechanics* 68: 721–738.

Hillgren VJ, Gessmann CK, and Li J (2000) An experimental perspective on the light element in Earth's core. In: Canup RM and Righter K (eds.) *Origin of the Earth and Moon*, pp. 245–264. Tucson, AZ: University of Arizona Press.

Humayun M, Qin L, and Norman MD (2004) Geochemical evidence for excess iron in the mantle beneath Hawaii. *Science* 306: 91–94.

Jacobs JA (1998) Variations in the intensity of the Earth's magnetic field. *Surveys in Geophysics* 19: 139–187.

Jephcoat A and Olson P (1987) Is the inner core of the Earth pure iron. *Nature* 325: 332–335.

Kanda RVS and Stevenson DJ (2006) Suction mechanism for iron entrainment into the lower mantle. *Geophysical Research Letters* 33: L02310.

Kellogg LH and King SD (1993) Effect of mantle plumes on the growth of D'' by reaction between the core and mantle. *Geophysical Research Letters* 20: 379–382.

Kilburn MR and Wood BJ (1997) Metal-silicate partitioning and the incompatibility of S and Si during core formation. *Earth and Planetary Science Letters* 152: 139–148.

Kleine T, Munker C, Mezger K, and Palme H (2002) Rapid accretion and early core formation on asteroids and the terrestrial planets from Hf-W chronometry. *Nature* 418: 952–955.

Knittle E (1998) The solid/liquid partitioning of major and radiogenic elements at lower mantle pressures: Implications for the core–mantle boundary region. In: Gurnis M, Wysession ME, Knittle E, and Buffet BA (eds.) *Geodynamics 28: The Core–Mantle Boundary Region*, pp. 119–130. Washington, DC: American Geophysical Union.

Knittle E and Jeanloz R (1991) Earth's core–mantle boundary – results of experiments at high pressures and temperatures. *Science* 251: 1438–1443.

Kono M and Roberts PH (2002) Recent geodynamo simulations and observations of the geomagnetic field. *Reviews of Geophysics* 40: 1013.

Koper KD and Dombrovskaya M (2005) Seismic properties of the inner core boundary from PKiKP/P amplitude ratios. *Earth and Planetary Science Letters* 237: 680–694.

Kuang WL and Bloxham J (1997) An Earth-like numerical dynamo model. *Nature* 398: 371–374.

Labrosse S (2002) Hotspots, mantle plumes and core heat loss. *Earth and Planetary Science Letters* 199: 147–156.

Labrosse S (2003) Thermal and magnetic evolution of the Earth's core. *Physics of the Earth and Planetary Interiors* 140: 127–143.

Labrosse S and Macouin M (2003) The inner core and the geodynamo. *Comptes Rendus Geoscience* 335: 37–50.

Labrosse S, Poirier JP, and Le Mouel JL (1997) On cooling of the Earth's core. *Physics of the Earth and Planetary Interiors* 99: 1–17.

Labrosse S, Poirier JP, and Le Mouel JL (2001) The age of the inner core. *Earth and Planetary Science Letters* 190: 111–123.

Laio A, Bernard S, Chiarotti GL, Scandolo S, and Tosatti E (2000) Physics of iron at Earth's core conditions. *Science* 287: 1027–1030.

Lassiter JC (2004) Role of recycled oceanic crust in the potassium and argon budget of the Earth: Toward a resolution of the ''missing argon'' problem. *Geochemistry Geophysics Geosystems* 5: Q11012.

Lassiter JC (2006) Constraints on the coupled thermal evolution of the Earth's core and mantle, the age of the inner core, and the origin of the Os-186 Os-188 'core signal' in plume-derived lavas. *Earth and Planetary Science Letters* 250: 306–317.

Layer PW, Kroner A, and McWilliams M (1996) An Archean geomagnetic reversal in the Kaap Valley pluton, South Africa. *Science* 273: 943–946.

Lee KKM and Steinle-Neumann G (2006) High-pressure alloying of iron and xenon: 'Missing' Xe in the Earth's core? *Journal of Geophysical Research* 111: B02202.

Lee KKM, Steinle-Neumann G, and Jeanloz R (2004) *Ab-initio* high-pressure alloying of iron and potassium: Implications for the Earth's core. *Geophysical Research Letters* 31: L11603.

Li J and Fei YW (2003) Experimental Constraints on Core Composition. In: Carlson RW (ed.) *Treatise on Geochemistry*, The Mantle and Core, vol. 2, pp. 521–546. Amsterdam: Elsevier.

Lister JR (2003) Expressions for the dissipation driven by convection in the Earth's core. *Physics of the Earth and Planetary Interiors* 140: 145–158.

Lister JR and Buffett BA (1998) Stratification of the outer core at the core–mantle boundary. *Physics of the Earth and Planetary Interiors* 105: 5–19.

Loper DE (1978) The gravitationally powered dynamo. *Geophysical Journal of the Royal Astronomical Society* 54: 389–404.

Lowrie W and Kent DV (2004) Geomagnetic polarity timescales and reversal frequency regimes. In: Channell JET, Kent, Lowrie W, and Meert J (eds.) *Geophysical Monograph 145*, Timescale of the Paleomagnetic Field, pp. 117–129. Washington, DC: American Geophysical Union.

Ma YZ, Somayazulu M, Shen GY, Mao HK, Shu JF, and Hemley RJ (2004) *In situ* X-ray diffraction studies of iron to Earth-core conditions. *Physics of the Earth and Planetary Interiors* 143: 455–467.

Malavergne V, Siebert J, Guyot F, *et al.* (2004) Si in the core? New high-pressure and high-temperature experimental data. *Geochemica et Cosmochimica Acta* 68: 4201–4211.

Manga M and Jeanloz R (1996) Implications of a metal-bearing chemical boundary layer in D'' for mantle dynamics. *Geophysical Research Letters* 23: 3091–3094.

Masters G and Gubbins D (2003) On the resolution of density within the Earth. *Physics of the Earth and Planetary Interiors* 140: 159–167.

Matassov G (1977) *The electrical conductivity of iron–silicon alloys at high pressures and the Earth's core*. PhD Thesis, Lawrence Livermore Laboratory, University of California, CA.

Matsuda J, Sudo M, Ozima M, Ito K, Ohtaka O, and Ito E (1993) Noble gas partitioning between metal and silicate under high pressures. *Science* 259: 788–790.

McDonough WF (2003) Compositional model for the Earth's core. In: Carlson RW (ed.) *Treatise on Geochemistry: The Mantle and Core*, pp. 517–568. Amsterdam: Elsevier.

McElhinny MW and Senanayake WE (1980) Paleomagnetic evidence for the existence of the geomagnetic field 3.5 Ga ago. *Journal of Geophysical Research* 85: 3523–3528.

Mittelstaedt E and Tackley PJ (2006) Plume heat flow is much lower than CMB heat flow. *Earth and Planetary Science Letters* 241: 202–210.

Mollett S (1984) Thermal and magnetic constraints on the cooling of the Earth. *Geophysical Journal of the Royal Astronomical Society* 76: 653–666.

Morgan JW and Anders E (1980) Chemical composition of the Earth, Venus and Mercury. *Proceedings of the National Academy of Sciences USA* 77: 6973–6977.

Morgan JW, Horan MF, Walker RJ, and Grossman JN (1995) Rhenium–osmium concentration and isotope systematics in Group IIAB iron meteorites. *Geochemica et Cosmochimica Acta* 59: 2331–2344.

Murakami M, Hirose K, Kawamura K, Sata N, and Ohishi Y (2004) Post-perovskite phase transition in $MgSiO_3$. *Science* 304: 855–858.

Murthy VR, van Westrenen W, and Fei YW (2003) Experimental evidence that potassium is a substantial radioactive heat source in planetary cores. *Nature* 323: 163–165.

Nakagawa T and Tackley PJ (2004a) Effects of thermo–chemical mantle convection on the thermal evolution of the Earth's core. *Earth and Planetary Science Letters* 220: 107–119.

Nakagawa T and Tackley PJ (2004b) Effects of a perovskite-post perovskite phase change near core–mantle boundary in compressible mantle convection. *Geophysical Research Letters* 31: 16611.

Nguyen JH and Holmes NC (2004) Melting of iron at the physical conditions of the Earth's core. *Nature* 427: 339–342.

Nielsen SG, Rehkamper M, Norman MD, Halliday AN, and Harrison D (2006) Thallium isotopic evidence for ferromanganese sediments in the mantle source of Hawaiian basalts. *Nature* 439: 314–317.

Nimmo F and Agnor CB (2006) Isotopic outcomes of N-body accretion simulations: Constraints on equilibration processes during large impacts from Hf-W observations. *Earth and Planetary Science Letters* 243: 26–43.

Nimmo F, Price GD, Brodholt J, and Gubbins D (2004) The influence of potassium on core and geodynamo evolution. *Geophysical Journal International* 156: 363–376.

Okuchi T (1997) Hydrogen partitioning into molten iron at high pressure: Implications for Earth's core. *Science* 278: 1781–1784.

Olson P and Christensen UR (2006) Dipole moment scaling for convection-driven planetary dynamos. *Earth and Planetary Science Letters* 250: 561–571.

Ostanin S, Alfe D, Dobson D, Vocadlo L, Brodholt JP, and Price GD (2006) *Ab initio* study of the phase separation of argon in molten iron at high pressures. *Geophysical Research Letters* 33: L06303.

Poirier J-P (1994) Light elements in the Earth's outer core: A critical review. *Physics of the Earth and Planetary Interiors* 85: 319–337.

Poirier J-P, Malavergene V, and Le Mouel JL (1998) Is there a thin electrically conducting layer at the base of the mantle? In: Gurnis M, Wysession ME, Knittle E, and Buffet BA (eds.) *Geodynamics 28: The Core–Mantle Boundary Region*, pp. 131–138. Washington, DC: American Geophysical Union.

Prevot M, Derder ME, McWilliams M, and Thompson J (1990) Intensity of the Earth's magnetic field – evidence for a Mesozoic dipole low. *Earth and Planetary Science Letters* 97: 129–139.

Puchtel IS, Brandon AD, Humayun M, and Walker RJ (2005) Evidence for the early differentiation of the core from Pt-Re-Os isotope systematics of 2.8-Ga komatiites. *Earth and Planetary Science Letters* 237: 118–134.

Righter K and Drake MJ (2003) Partition coefficients at high pressure and temperature. In: Carlson RW (ed.) *Treatise on Geochemistry, vol. 2: The Mantle and Core*, pp. 425–449. Amsterdam: Elsevier.

Roberts PH and Glatzmaier GA (2001) The geodynamo, past, present and future. *Geophysical and Astrophysical Fluid Dynamics* 94: 47–84.

Roberts PH, Jones CA, and Calderwood A (2003) Energy fluxes and Ohmic dissipation in the Earth's core. In: Jones CA, Soward AM, and Zhang K (eds.) *Earth's Core and Lower Mantle*, pp. 100–129. New York: Taylor & Francis.

Schersten A, Elliott T, Hawkesworth C, and Norman M (2004) Tungsten isotope evidence that mantle plumes contain no contribution from the Earth's core. *Nature* 427: 234–237.

Selkin PA and Tauxe L (2000) Long-term variations in palaeointensity. *Philosophical Transactions of the Royal Society of London A* 358: 1065–1088.

Shen GY, Mao HK, Hemley RJ, Duffy TS, and Rivers ML (1998) Melting and crystal structure of iron at high pressures and temperatures. *Geophysical Research Letters* 25: 373–376.

Sleep NH (1988) Gradual entrainment of a chemical layer at the base of the mantle by overlying convection. *Geophysical Journal International* 95: 437–447.

Sleep NH (1990) Hot spots and mantle plumes: Some phenomenology. *Journal of Geophysical Research* 95: 6715–6736.

Stacey FD and Anderson OL (2001) Electrical and thermal conductivities of Fe–Ni–Si alloy under core conditions. *Physics of the Earth and Planetary Interiors* 124: 153–162.

Stacey FD and Loper DE (1984) Thermal histories of the core and mantle. *Physics of the Earth and Planetary Interiors* 36: 99–115.

Stevenson DJ, Spohn T, and Schubert G (1983) Magnetism and thermal evolution of the terrestrial planets. *Icarus* 54: 466–489.

Sumita I and Yoshida S (2003) Thermal interactions between the mantle, outer and inner cores, and the resulting structural evolution of the core. In: Dehant V, Creager K, Zatman S, and Karato S-I (eds.) *Geodynamics Series 31: Earth's Core: Structure, Dynamics and Rotation*, pp. 213–231. Washington, DC: American Geophysical Union.

Tolstikhin I and Hofmann AW (2005) Early crust on top of the Earth's core. *Physics of the Earth and Planetary Interiors* 148: 109–130.

Turcotte DL and Schubert G (2002) *Geodynamics*. New York: Cambridge University Press.

Valet JP (2003) Time variations in geomagnetic intensity. *Reviews of Geophysics* 41: 1004.

Verhoogen J (1961) Heat balance of the Earth's core. *Geophysical Journal of the Royal Astronomical Society* 4: 276–281.

Walker D (2000) Core participation in mantle geochemistry. *Geochemica et Cosmochimica Acta* 64: 2897–2911.

Walker RJ, Morgan JW, and Horan MF (1995) Os-187 enrichment in some plumes: Evidence for core–mantle interaction?. *Science* 269: 819–822.

Wanke H and Dreibus G (1988) Chemical composition and accretion history of terrestrial planets. *Philosophical Transactions of the Royal Society of London* 325: 545–557.

Williams Q (1998) The temperature contrast across D″. In: Gurnis M, Wysession M, Knittle E, and Buffett B (eds.) *Geodynamics*, 28, *The Core–Mantle Boundary Region*, pp. 73–82. Washington, DC: American Geophysical Union.

Yoo CS, Holmes NC, Ross M, Webb DJ, and Pike C (1993) Shock temperatures and melting of iron at Earth core conditions. *Physical Review Letters* 70: 3931–3934.

Yukutake T (2000) The inner core and the surface heat flow as clues to estimating the initial temperature of the Earth's core. *Physics of the Earth and Planetary Interiors* 121: 103–137.

Zhong S (2006) Constraints on thermochemical convection of the mantle from plume heat flux, plume excess temperature and upper mantle temperature. *Journal of Geophysical Research* 111: B04409.